Preparation, Aromaticity, and Bromination of Spiro Iridafurans

Miguel A. Esteruelas, Félix Leon, Sonia Moreno-Blázquez, Montserrat Oliván, and Enrique Oñate*

Departamento de Química Inorgánica - Instituto de Síntesis Química y Catálisis Homogénea (ISQCH) - Centro de Innovación en Química Avanzada (ORFEO-CINQA), Universidad de Zaragoza - CSIC, 50009 Zaragoza, Spain

ABSTRACT

Iridium centers of $[Ir(\mu\text{-}Cl)(C_8H_{14})_2]_2$ (**1**) activate the $C_\beta(sp^2)$-H bond of benzylideneacetone to give $[Ir(\mu\text{-}Cl)\{\kappa^2\text{-}C,O\text{-}[C(Ph)CHC(Me)O]\}_2]_2$ (**2**), which is the starting point for the preparation of the spiro iridafurans $IrCl\{\kappa^2\text{-}C,O\text{-}[C(Ph)CHC(Me)O]\}_2(P^iPr_3)$ (**3**), $[Ir\{\kappa^2\text{-}C,O\text{-}[C(Ph)CHC(Me)O]\}_2(MeCN)_2]BF_4$ (**4**), $[Ir(\mu\text{-}OH)\{\kappa^2\text{-}C,O\text{-}[C(Ph)CHC(Me)O]\}_2]_2$ (**5**), $Ir\{\kappa^2\text{-}C,O\text{-}[C(Ph)CHC(Me)O]\}_2\{\kappa^2\text{-}C,N\text{-}[C_6MeH_3\text{-}py]\}$ (**6**), and $Ir\{\kappa^2\text{-}C,O\text{-}[C(Ph)CHC(Me)O]\}_2\{\kappa^2\text{-}O,O\text{-}[acac]\}$ (**7**). The five-membered rings are orthogonally arranged with the oxygen atoms in *trans*, in an octahedral environment of the iridium atom. Spiro iridafurans are aromatic. The degree of aromaticity and the negative charge of the CH-carbon of the rings depend on the ligand *trans* to the carbon directly attached to the metal. Aromaticity has been experimentally confirmed by bromination of the iridafurans with *N*-bromosuccinimide (NBS). Reactions are sensitive to the

degree of aromaticity of the ring and the negative charge of the attacked CH-carbon. Iridafurans can be selectively brominated, when different ligands lie *trans* to metallated carbons. Bromination of **3** occurs in the ring with the metallated carbon *trans* to chloride, whereas the bromination of **6** takes place in the ring with the metallated carbon *trans* to pyridyl. The first gives IrCl{κ^2-*C,O*-[C(Ph)CBrC(Me)O]}{κ^2-*C,O*-[C(Ph)CHC(Me)O]}(P^iPr_3) (**8**), which reacts with more NBS to form IrCl{κ^2-*C,O*-[C(Ph)CBrC(Me)O]}$_2$(P^iPr_3) (**9**). The second yields Ir{κ^2-*C,O*-[C(Ph)CBrC(Me)O]}{κ^2-*C,O*-[C(Ph)CHC(Me)O]}{κ^2-*C,N*-[C_6MeH_3-py]} (**10**). The origin of the selectivity is kinetic, the rate-determining step of the reaction being the NBS attack. The activation energy depends on the negative charge of attacked atom; a higher negative charge allows for a lower activation energy. Accordingly, complex **7** undergoes bromination in the acetylacetonate ligand, giving Ir{κ^2-*C,O*-[C(Ph)CHC(Me)O]}$_2${κ^2-*O,O*-[acacBr]} (**11**).

INTRODUCTION

The substitution of a CH unit of an aromatic organic molecule by a transition metal and its associated ligands, maintaining the aromatic nature, endows the resulting molecule with organometallic properties. This simple principle has given rise to one of the most fascinating fields in chemistry today: metallaromatic compounds. Its origins go back to 1982, when Roper's group provided experimental evidence for the theoretical prediction of the existence of aromatic metallacycles, made by Thorn and Hoffmann in 1979,[1] with the preparation of the first osmabenzene.[2] Since then, a wide range of aromatic species of this class have been isolated,[3] mainly metallahydrocarbons[4] and, to a lesser extent, metallaheterocycles[5] and metalladiheterocycles.[6] As a consequence of the effort, the field has now reached a remarkable degree of conceptual maturity.[7]

Transition metals possess an incomplete *d* subshell, with shapes and orientations of the *d* orbitals that allow infeasible bonding patterns for the *s* and *p* orbitals; for example, spiroaromaticity.[8] Purely organic spiro polycyclic aromatic compounds are those formed by two conjugated π-systems, fixed perpendicularly by a sp^3 spiro carbon that does not intervene in electronic delocalization.[9] When this spiro carbon atom is replaced by a transition metal atom, it may itself be involved in electron delocalization, thus forming spiro aromatic compounds.[3l] The rings can maintain aromaticity independently or join together to show overall aromaticity. Thus three types of lithium-stabilized aromatic spiro metallahydrocarbons have been isolated and characterized: square-planar,[10] orthogonal,[11] and tricyclic-octahedral[12] (**I**, **II**, and **III**, respectively in Chart 1). In addition, Jia's group has recently reported the existence of a fascinating spiro rhenacyclopropene derivative that exhibits σ-aromaticity.[13]

Chart 1. Lithium-Stabilized Aromatic Spiro Metallahydrocarbons

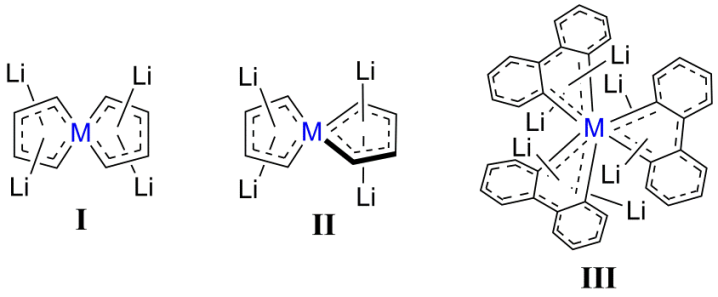

Aromatic metallaheterocycles are a relevant subclass of metallaromatic compounds containing a main group heteroatom.[3j] Thus, one further step in the field is to extend spiroaromaticity to the spiro compounds of said subclass. The metallafurans are probably the most numerous among the aromatic metallaheterocycles.[14] However, spiro metallacycles of this type are very rare and were not described as aromatic species at the time of publication. To the best of our knowledge, only two previous reports show compounds that could currently be considered aromatic spiro furans. In

2005, Crabtree's group reported that the insertion of the C-C triple bond of activated alkynes, HC≡CC(O)R (R = Me, OMe), into the Ir-H bond of the hydride-iridafuran [IrH{κ^2-*C,O*-[C(Ph)CHC(Me)O]}(PPh$_3$)$_2${κ^1-*O*-[O=CMe$_2$]}]$^+$ cation produced a second iradafuran cycle arranged orthogonally to the first, with the oxygen atoms in *cis*. In refluxing acetonitrile, the bicyclic system undergoes a rearrangement to place the monocycles in the same plane (Scheme 1a).[15] Three years later, we showed that C-H bond activation of two methyl vinyl ketone molecules promoted by a hydride-osmium(II)-(elongated dihydrogen) complex gives a bifuran system with a spiro-[OsH(P^{i}Pr$_3$)$_2$]$^+$ metal fragment. The metal center of this unit is capable of being deprotonated to afford a neutral spiro-[Os(P^{i}Pr$_3$)$_2$] moiety. The monocycles lie in the same plane in both spiro arrangements, in contrast to the case of iridium (Scheme 1b).[16]

Scheme 1. Preparation of Previously Reported Spiro Metallafurans

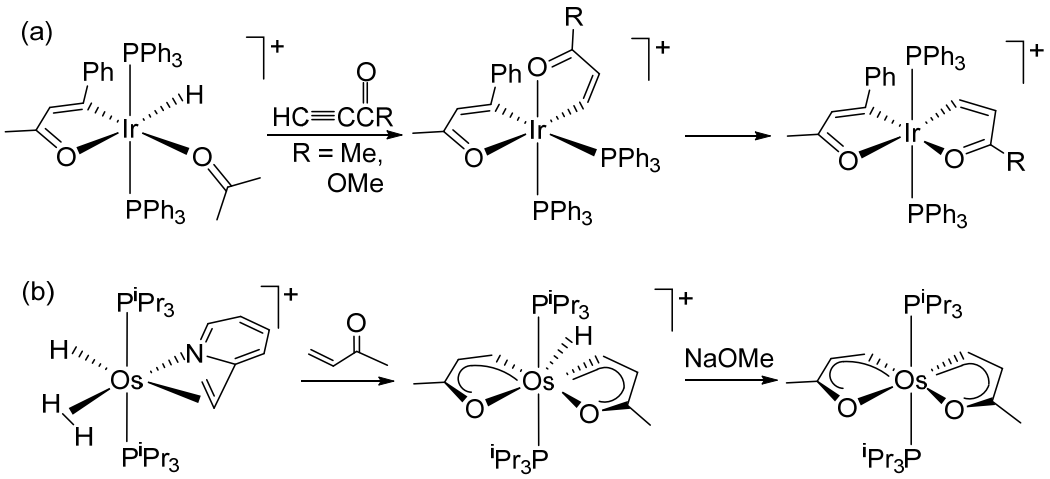

The aromaticity of metallaromatic compounds has been evaluated mainly by computational methods. They include calculation of Aromatic Stabilization Energy (ASE),[17] Nucleus Independent Chemical Shift (NICS)[18] and Anisotropy of the Induced Current Density (AICD)[19] and, to a lesser extent, Natural Bonding Orbital (NBO)[20] analysis. The experimental criteria are

mainly based on X-ray diffraction analysis and include the degree of planarity of the metallacycle and the equalization of the bond lengths. On the other hand, the effort made in the analysis of the reactivity of these organometallic compounds and their comparison with that of purely organic molecules has been scarce.[6a,d;21] In this context, it should be pointed out that electrophilic aromatic substitution reactions are a characteristic of aromatic compounds.[22] Halogenation is undoubtedly one of the most important, partly because aromatic halides are basic components in organic synthesis, especially with the advent of cross-coupling reactions.[23] Because the strength of C-halide bonds decreases as we go down in group 17 of the periodic table, bromination is of special interest.[24] They begin with electrophile attack on the aromatic ring to generate a delocalized cyclic cation containing a strongly acidic $C(sp^3)$-H moiety. This group donates the proton to the solvent or any other weak base, to restore aromaticity around the entire ring again. The net result is the substitution of a hydrogen atom by the electrophile.[22] Oxygen atom of furans substantially stabilizes the cationic intermediate. As a consequence, furans are kinetically more susceptible to bromination than benzene and related hydrocarbons.[25] In other words, the easy bromination of spiro metallafurans should be further evidence of their aromaticity.

This paper reports on the preparation of a family of orthogonal spiro iridafurans with the oxygen atoms in *trans*. It demonstrates the spiroaromaticity of this type of metallaheterocycles while analyzing the degree of aromaticity of each independent monocycle, including its ability to undergo selective bromination, as a function of the nature of the L ligands of the spiro-[IrL_2] metal fragment.

RESULTS AND DISCUSSION

Members of the Discovered Family of Spiro Iridafurans. The starting point of this family is the reaction of the well-known iridium(I)-olefin precursor $[Ir(\mu\text{-}Cl)(C_8H_{14})_2]_2$ (**1**) with benzylideneacetone (Scheme 2). This complex releases the olefins and activates the $C\beta(sp^2)$-H bond of four ketone molecules to give the iridium(III)-dimer $[Ir(\mu\text{-}Cl)\{\kappa^2\text{-}C,O\text{-}[C(Ph)CHC(Me)O]\}_2]_2$ (**2**) as red crystals in 79% yield. The activations were achieved in the molten ketone, at 100 ºC, for 4 h.

Scheme 2. Preparation of Complex 2

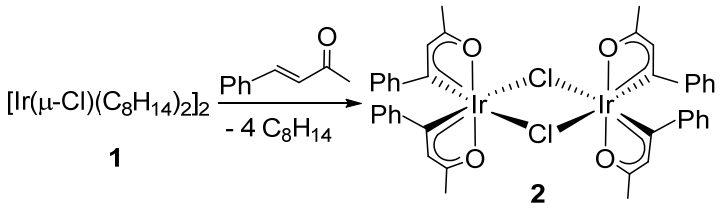

Complex **2** was characterized by X-ray diffraction analysis. The structure (Figure 1) proves the C-H bond activations and the spiro-furanic nature of the mononuclear fragments, showing an eclipsed arrangement between the spiro sequences. In each mononuclear half, the planar iridafuran rings are located orthogonally forming dihedral angles between them of 85.80(11)º (Ir(1)) and 87.31(11)º (Ir(2)). The iridium centers lie in an octahedral environment. In contrast to the spiro metallafuran derivatives of Scheme 1, the oxygen atoms of the five-membered metallarings are mutually *trans* (O(1)-Ir(1)-O(1A) = 178.88(17)º and O(2)-Ir(2)-O(2A) = 179.76(17)º), while the carbon atoms are arranged *trans* to the chloride bridges (C(1)-Ir(1)-Cl(1A) = C(1A)-Ir(1)-Cl(1) = 171.94(13)º and C(11)-Ir(2)-Cl(1A) = C(11A)-Ir(2)-Cl(1) = 169.47(13)º).

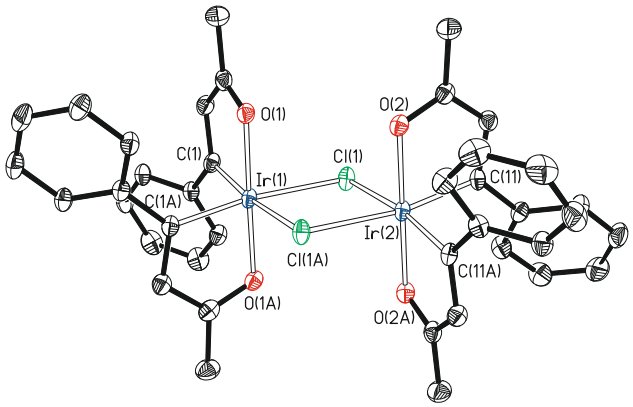

Figure 1. Molecular diagram of complex **2** (displacement ellipsoids shown at 50% probability). All hydrogen atoms are omitted for clarity. Selected bond distances (Å) and angles (deg): Ir(1)-Cl(1) = Ir(1)-Cl(1A) = 2.4809(10), Ir(2)-Cl(1) = Ir(2)-Cl(1A) = 2.4753(10), Ir(1)-C(1) = Ir(1)-C(1A) = 1.986(4), Ir(2)-C(11) = Ir(2)-C(11A) = 1.986(4), Ir(1)-O(1) = Ir(1)-O(1A) = 2.040(3), Ir(2)-O(2) = Ir(2)-O(2A) = 2.039(3); O(1)-Ir(1)-O(1A) = 178.88(17), O(2)-Ir(2)-O(2A) = 179.76(17), C(1)-Ir(1)-Cl(1A) = C(1A)-Ir(1)-Cl(1) = 171.94(13), C(11)-Ir(2)-Cl(1A) = C(11A)-Ir(2)-Cl(1) = 169.47(13), O(1)-Ir(1)-C(1) = O(1A)-Ir(1)-C(1A) = 80.53(16), O(2)-Ir(2)-C(11) = O(2A)-Ir(2)-C(11A) = 80.21(15).

Molecule **2** ideally belongs to the C_{2h} symmetry group, with the C_2 axis connecting the metal centers while the perpendicular plane contains the chloride bridges. These elements of symmetry balance the five-membered rings. Accordingly, the ^{1}H and $^{13}C\{^{1}H\}$ NMR spectra of the red crystals, in dichloromethane-d_2, at room temperature show resonances for only one type of iridafuran; the most notable signals are a singlet at 6.54 ppm in ^{1}H, corresponding to the equivalent CH-hydrogen atoms, and another singlet in $^{13}C\{^{1}H\}$ at 217.4 ppm due to the carbon atoms attached directly to the iridium centers. In toluene, at 100 °C, the metallated carbon atoms of one of the mononuclear moieties exchange their positions to give the alternated isomer **2a**, with the spiro rings of these halves offset from one another (Scheme 3). This isomer belongs to the D_2 symmetry

group, defined by three perpendicular C_2 axes which intersect at the center of the Ir_2Cl_2 core and also balance the iridafuran rings. In the ^1H NMR spectrum, the resonance corresponding to the CH-hydrogen atom of the five-membered rings of the new isomer is observed slightly shifted to lower field with respect to that of **2**, 6.34 *versus* 6.31 ppm in toluene-d_8 (Figure S3). For its part, the $^{13}C\{^1H\}$ NMR spectrum contains the signal due to the carbon atom attached to the metal at 216.5 ppm. Density functional theory (DFT) calculations (B3LYP-D3//SDD(f)/6-31G**) reveal that the isomers have the same stability (Figure S27). Consequently, the NMR spectra of the red crystals contain characteristic signals of both, in the same intensity ratio, after 16 h.

Scheme 3. Isomerization of Complex 2

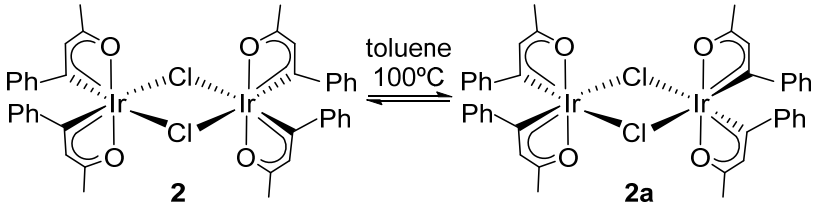

Complex **2** is a new member of the $[Ir(\mu\text{-}Cl)(3b)_2]_2$ (3b = 3e donor bidentate ligand) class of compounds,[26] where orthometallated 2-phenylpyridine-type groups are the most common 3b ligands.[27] Its reactivity is consistent with such lineage, chloride bridges can be cleaved with monodentate 2e donor ligands, abstracted with silver salts in the presence of coordinating solvents, or replaced by other 3e donor ligands such as the hydroxide group (Scheme 4). At room temperature, complex **2** reacts with triisopropylphosphine in dichloromethane to give $IrCl\{\kappa^2\text{-}C,O\text{-}[C(Ph)CHC(Me)O]\}(P^iPr_3)$ (**3**), with $AgBF_4$ in acetonitrile to afford $[Ir\{\kappa^2\text{-}C,O\text{-}[C(Ph)CHC(Me)O]\}_2(MeCN)_2]BF_4$ (**4**), and with aqueous KOH in acetone to form $[Ir(\mu\text{-}OH)\{\kappa^2\text{-}C,O\text{-}[C(Ph)CHC(Me)O]\}_2]_2$ (**5**). Complex **3** was isolated as an orange solid in 84% yield, whereas the salt **4** was obtained as a yellow solid in almost quantitative yield. The latter is a synthetic

intermediate, which allows to prepare heteroleptic species with a third 3e donor asymmetric *C,N*-ligand of orthometallated 2-phenylpyridine-type, by heterolytic activation of an *ortho*-CH bond of the heterocycle substituent. Thus, treatment of solutions of **4**, in fluorobenzene, with 2-(*p*-tolyl)pyridine, in the presence of the external base (piperidinomethyl)polystyrene, under reflux leads to Ir{κ^2-*C,O*-[C(Ph)CHC(Me)O]}$_2${κ^2-*C,N*-[C_6MeH_3-py]} (**6**), as a red solid in 83% yield. Dimer **5**, was obtained as a red solid in almost quantitative yield. In contrast to **2,** complex **5** decomposes in toluene at 100 ºC. It is also a synthetic intermediate, since the hydroxide bridges can be replaced by chelating ligands through the protonation of the bridges with pro-ligands bearing acidic hydrogen atoms, as for example acetylacetone (Hacac). Addition of 5.0 equiv of the diketone to suspensions of **5** in acetone gives Ir{κ^2-*C,O*-[C(Ph)CHC(Me)O]}$_2${κ^2-*O,O*-[acac]} (**7**), which was isolated as a red solid in almost quantitative yield. Complex **7** can be directly obtained from **2**, by reaction of the latter with Na(acac) in dichloromethane.

Scheme 4. Members of the Discovered Family

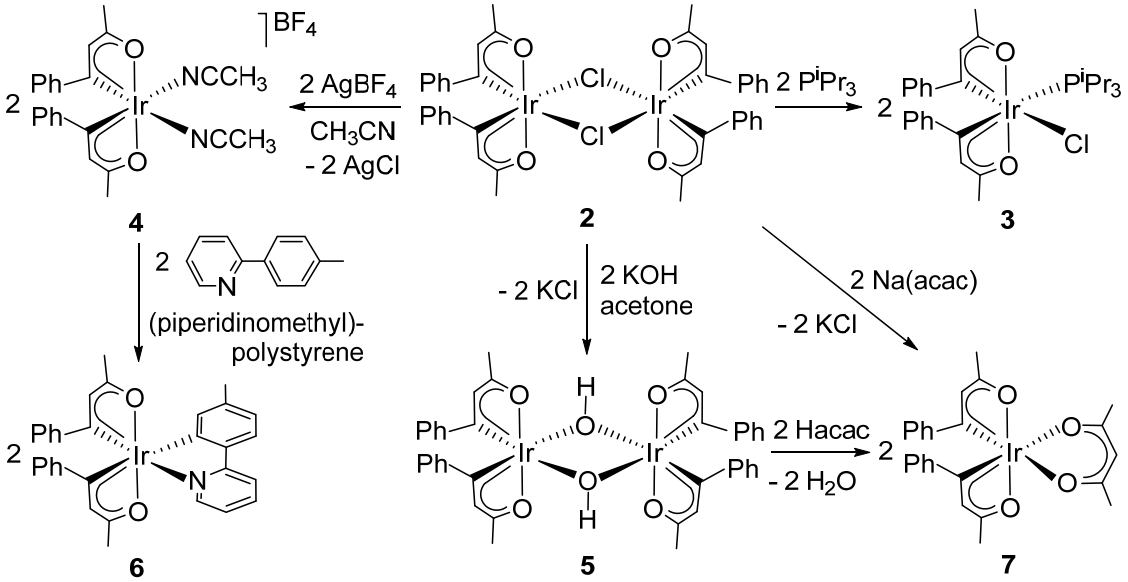

Complexes **3** and **4** were characterized by X-ray diffraction analysis. The most noticeable feature of the structures is the retention of the stereochemistry of the mononuclear fragments of **2**, as is usual in the reactions of $[Ir(\mu\text{-}Cl)(3b)_2]_2$ dimers.[28] Thus, the iridafuran rings are located orthogonally (dihedral angles: 78.48(4)º for **3** and 86.8(1) and 83.1(1) for **4**[29]), with the oxygen atoms situated mutually *trans* (O(1)-Ir-O(2) = 174.79(4)º for **3** and 176.64(19) and 179.6(2) for **4**). In an octahedral environment of the iridium atom, the structure of **3** (Figure 2) shows two inequivalent iridafuran rings with the metallated carbon atoms *trans* arranged to the monodentate ligands (C(1)-Ir-Cl = 166.28(4)º and C(11)-Ir-P(1) = 169.52(4)º), whereas the structure of the cation of **4** (Figure 3) displays two equivalent iridafurans with the metallated carbon atoms *trans* disposed to the nitrile molecules (C(1)-Ir-N(1) = 172.25(18) and 173.01(19)). The ^{1}H and $^{13}C\{^{1}H\}$ NMR spectra of **3-7**, in dichloromethane-d_2, at room temperature are consistent with these structures and agree well with those of **2**. Thus, the ^{1}H spectra contain one (**4**, **5**, and **7**) or two (**3** and **6**) signals between 6.5 and 7.0 ppm, due to the iridafuran CH-hydrogen atom, whereas the $^{13}C\{^{1}H\}$ spectra show one (**4**, **5**, and **7**) or two (**3** and **6**) signals at about 220 ppm corresponding to the metallated carbon atoms of the five-membered metallarings.

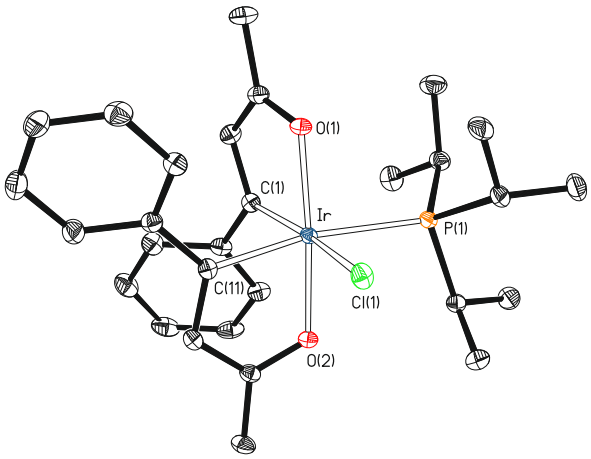

Figure 2. Molecular diagram of complex **3** (displacement ellipsoids shown at 50% probability). All hydrogen atoms are omitted for clarity. Selected bond distances (Å) and angles (deg): Ir-P(1) = 2.4097(4), Ir-Cl(1) = 2.4633(3), Ir-O(1) = 2.0518(10), Ir-O(2) = 2.0455(10), Ir-C(1) = 1.9768(14), Ir-C(11) = 2.0547(14); O(1)-Ir-C(1) = 79.75(5), O(2)-Ir-C(11) = 79.17(5), O(1)-Ir-O(2) = 174.79(4), Cl(1)-Ir-C(1) = 166.28(4), P(1)-Ir-C(1) = 104.43(4), P(1)-Ir-C(11) = 169.52(4), Cl(1)-Ir-C(11) = 85.55(4), O(1)-Ir-C(11) = 97.94(5), O(2)-Ir-C(1) = 95.52(5), O(2)-Ir-Cl(1) = 88.72(3), O(1)-Ir-Cl(1) = 95.40(3).

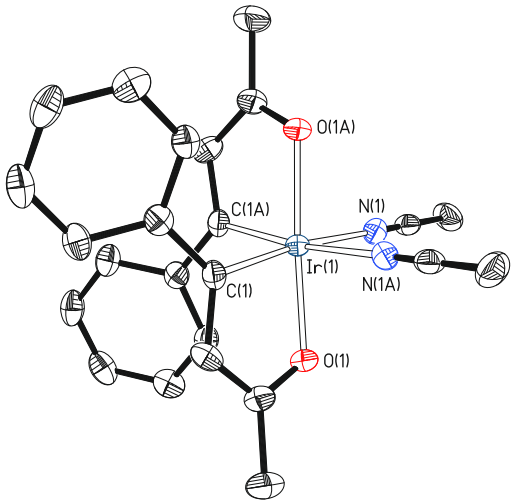

Figure 3. Molecular diagram of one of the two chemically equivalent but crystallographically independent cations of **4** (displacement ellipsoids shown at 50% probability). All hydrogen atoms are omitted for clarity. Selected bond distances (Å) and angles (deg): Ir(1)-C(1) = 1.999(5), 1.995(5), Ir(1)-O(1) = 2.033(3), 2.038(3), Ir(1)-N(1) = 2.094(5), 2.097(4); O(1)-Ir(1)-O(1A) = 176.64(19), 179.6(2), C(1)-Ir(1)-N(1) = 172.25(18), 173.01(19), C(1)-Ir(1)-O(1) = 80.52(17), 80.41(18), C(1)-Ir-C(1A) = 88.2(3), 86.4(3), N(1)-Ir(1)-N(1A) = 91.6(2), 90.8(2), O(1)-Ir(1)-N(1) = 92.25(15), 93.30(15), C(1)-Ir(1)-O(1A) = 101.93(17), 99.91(18).

Aromaticity Analysis. Structural criterion supports the aromaticity of the spiro rings. Structures of **2-4** reveal that the iridafurans are planar. The maximum deviation of the atoms forming the five-membered rings, from the best plane that passes through them, shows extremely small values in all cases (Table S1). Chart 2 collects bond lengths in the rings. They were obtained from the X-ray analysis for **2-4** or correspond to the optimized structures calculated by DFT for **2-4**, **6**, and **7**. In agreement with the existence of electron delocalization, the values are intermediate between those corresponding to single and double bonds. Furthermore, they indicate that to describe the bonding situation in the rings the alkylidene f_1 and alkenyl f_2 resonance forms must be taken into account (Scheme 5).

Chart 2. Bond Lengths (X-ray, blue; DFT, black; Å) in the Iridafuran Rings of Complexes 2 (a), 3 (b_1 and b_2), 4 (c), 6 (d_1 and d_2), and 7 (e).

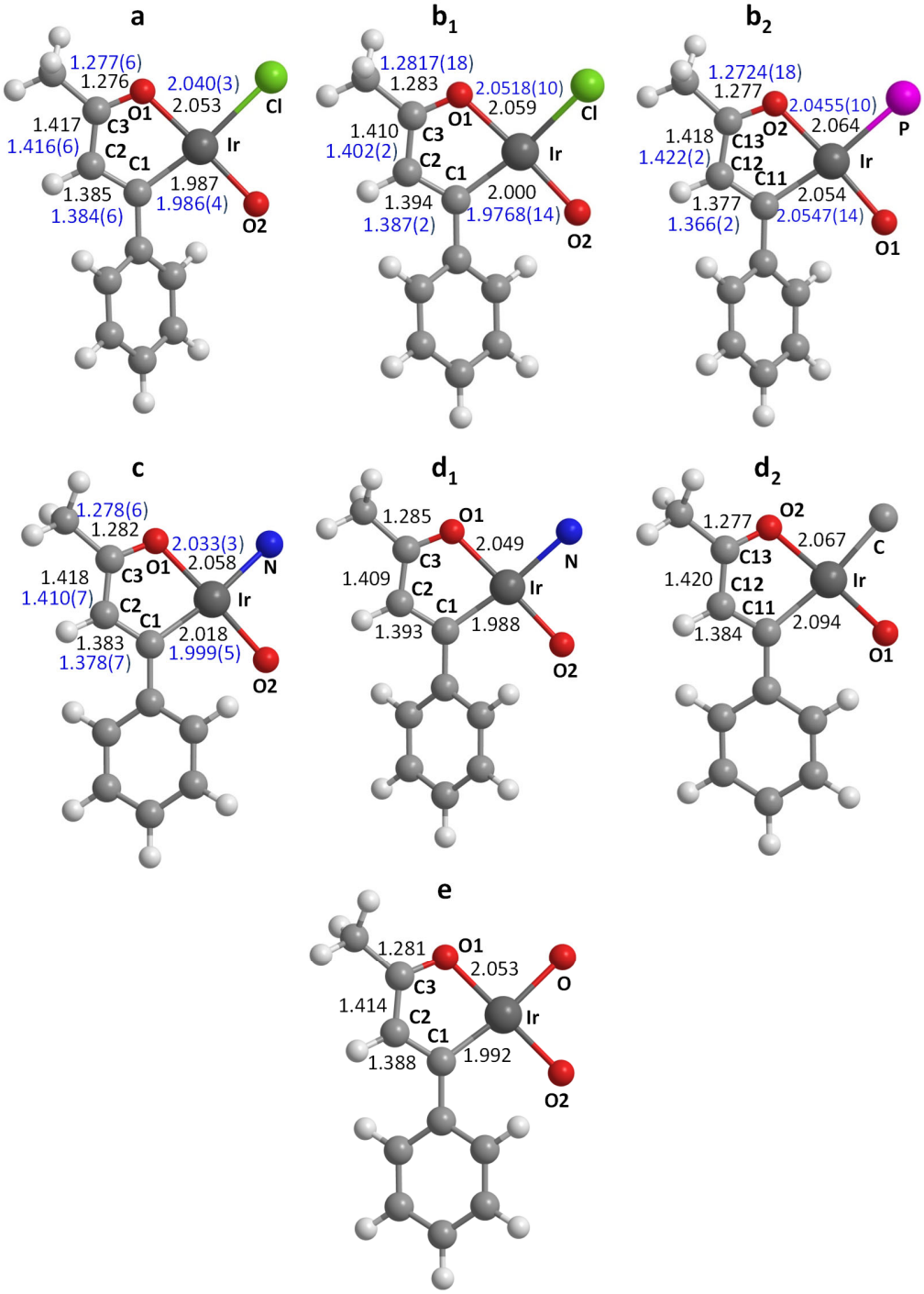

Scheme 5. Resonance Forms

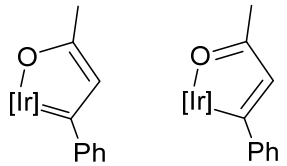

f_1 f_2

The NBO analysis yields Wiberg bond indices that are consistent with the existence of such electron delocalization (Chart 3). Indices also point out the sites where electron concentration occurs. The highest values correspond to bonds C(1)-C(2) and C(3)-O(1) of **2**, **4**, and **7** and C(1)-C(2) and C(3)-O(1) (**b**$_1$ and **d**$_1$) and C(11)-C(12) and C(13)-O(2) (**b**$_2$ and **d**$_2$) of the asymmetrical spiro rings of **3** and **6**. The electron concentration in these bonds suggests a predominant contribution of the f_2 resonance form to iridafurans, which is compatible with the localization of the π-orbitals of the rings (Figures S48-S52). Its contribution degree depends mainly on the group arranged *trans* to the carbon atom directly attached to the metal center. For the asymmetrical spiro iridafurans of **3** and **6,** the contribution degree is significantly bigger for the ring that disposes the metallated carbon atoms *trans* to the phosphine ligand and the orthometallated *p*-tolyl group, respectively; i. e., the contribution of f_2 to **b**$_2$ and **d**$_2$ is bigger than to **b**$_1$ and **d**$_1$.

Chart 3. Wiberg Bond Indices in the Iridafuran Rings of Complexes 2 (a), 3 (b_1 and b_2), 4 (c), 6 (d_1 and d_2), and 7 (e).

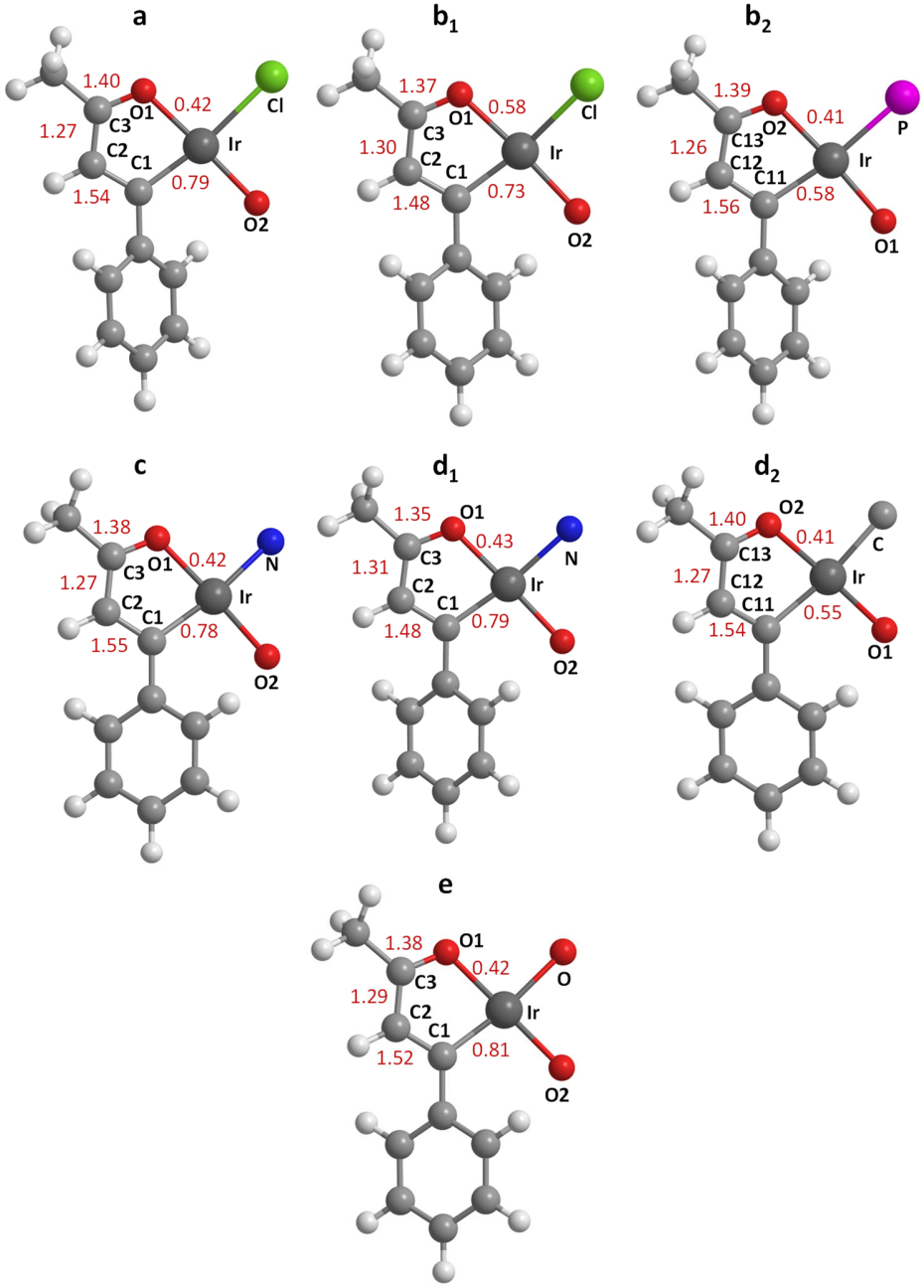

The NBO charges, also called NPA charges, on the atoms (Chart 4) reveal a remarkable negative character of C(2) and C(12), with values that are also refined by the group arranged *trans* to the carbon atom directly attached to the metal. For the asymmetrical spiro iridafurans of **3** and **6**, the

most negative values correspond to the carbons of the rings with smaller contribution of f_2; i. e., those with the metallated carbon atom arranged *trans* to the chloride ligand and to the pyridyl group (C2 of **b**$_1$ and **d**$_1$).

Chart 4. NBO charges in the irididdafuran rings of complexes 2 (a), 3 (b$_1$ and b$_2$), 4 (c), 6 (d$_1$ and d$_2$), and 7 (e).

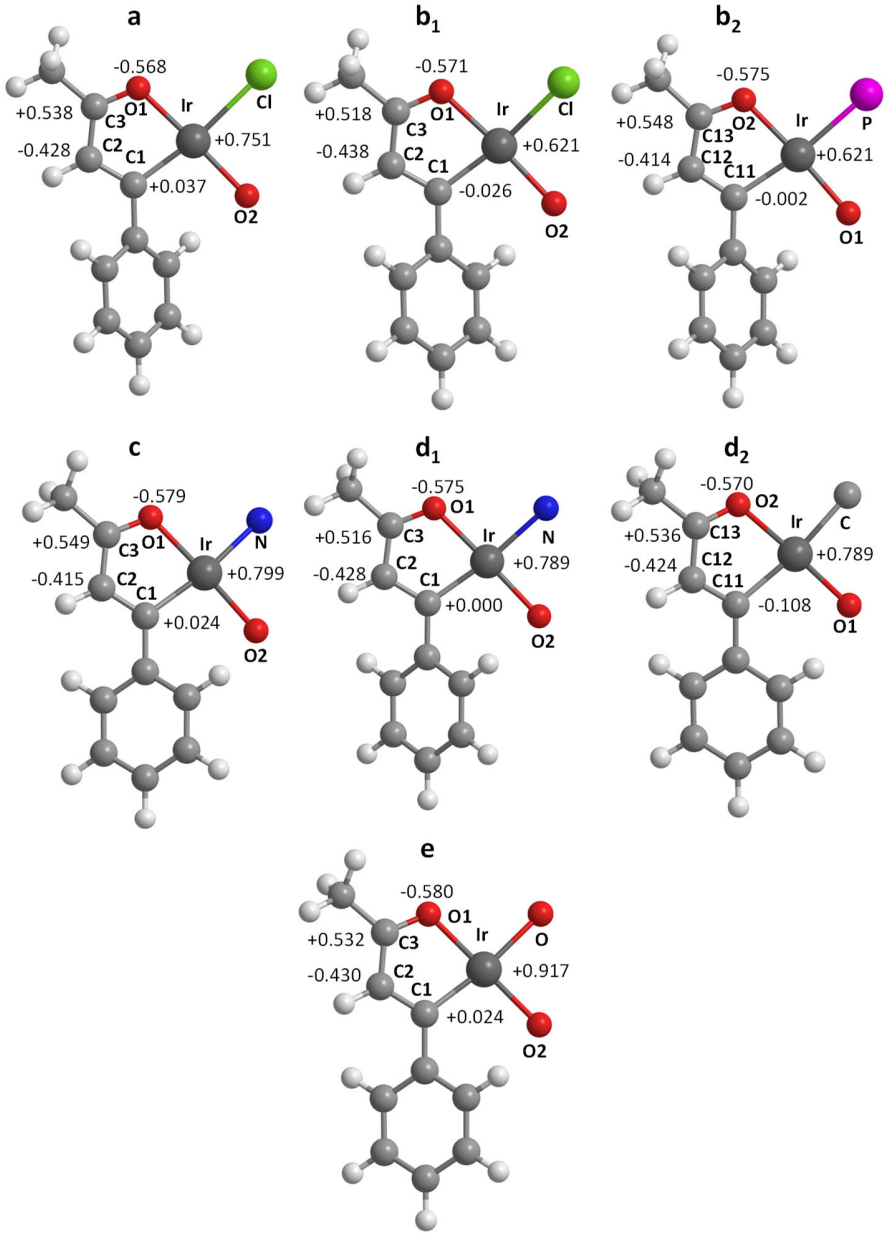

The AICD and NICS computational methods also support the aromaticity of spiro iridafurans. The respective AICD plots clearly show the appearance of a diatropic ring current (clockwise vectors) within the rings (Figures S30-S34), whereas the NICS and $NICS_{zz}$ scans (Figures S39-S43) provide values in the center of the rings and out of plane at 1 Å above and below that are consistent with aromaticity (Table 1). The most negative values are observed for **3**, especially for the iridafuran that has the metallated carbon atom *trans* disposed to the chloride ligand (**b_1**), and the ring of **6** with the metallated carbon atom located in the *trans* position to the pyridyl group (**d_1**). The bonding of these rings has precisely the lower contribution from the f_2 resonance form. Since the latter is the main contribution to the bond structure of the rings and its decrease implies an increase in the contribution of the f_1 resonance form, the coincidence of both findings on the same rings indicates that the NICS values are more negative when the respective contributions approach.

Table 1. NICS and NICSzz values in the center of the rings and out of plane at 1 Å above and below for complexes **2-4** and **6-11**

Complex	Ring[a]	NICS			NICSzz		
		0	1	-1	0	1	-1
2		-0.89	-2.96	-2.04	14.36	-6.15	-4.09
3	C *trans* to Cl	-3.74	-4.92	-3.62	5.09	-12.26	-11.16
	C *trans* to P	-2.80	-3.59	-3.37	11.52	-7.76	-7.47
4		-1.66	-2.83	-2.53	14.92	-6.00	-3.75
6	C *trans* to N	-2.67	-3.36	-2.93	9.85	-9.57	-7.92
	C *trans* to C	-0.63	-2.60	-1.46	12.10	-6.84	-5.13
7		-0.65	-3.02	-1.44	13.36	-7.39	-3.38
8	C *trans* to Cl	-4.00	-4.13	-3.89	7.78	-11.54	-10.32
	C *trans* to P	-2.17	-3.74	-3.15	12.39	-9.05	-6.03
9	C *trans* to Cl	-4.04	-4.28	-3.89	7.75	-12.22	-10.36
	C *trans* to P	-3.25	-4.05	-3.38	11.04	-9.01	-5.56
10	C *trans* to N	-4.06	-4.05	-3.09	8.60	-10.71	-7.84

	C *trans* to C	-0.74	-2.98	-1.44	11.33	-8.86	-5.49
11		-0.68	-3.01	-1.44	13.53	-7.38	-3.32

[a] C *trans* to X (X = Cl, P, N, C) denotes the C metallated carbon of the iridafuran disposed *trans* to X.

The ASE method provides additional computational evidence for the aromatic character of spiro iridafurans derivatives. We focused on hypothetical species resulting from the replacement of the CH-hydrogen atom of the five-membered rings of **3** and **6** by a methyl group. The replacement affords **3t** and **6t**, respectively. These particular examples were selected because they allow a fine analysis of the influence of the group arranged *trans* to the carbon atom directly attached to the metal, on the aromaticity of the ring. We studied the loss of stability that occurs, as a consequence of the dearomatization of the five-membered rings, when a hydrogen of said methyl group undergoes a 1,3-migration to the PhC-carbon atom of the ring. Thus, for **3t**, the isomerization of the iridafuran with the metallated carbon atom *trans* arranged to the chloride ligand gives **3t'$_1$**, whereas the isomerization of the ring with the metallated carbon atom disposed *trans* to the phosphine leads to **3t'$_2$**. The same process for **6t** gives rise to **6t'$_1$** (C trans to pyridyl) and **6t'$_2$** (C trans to *p*-tolyl). The loss of stability by dearomatizacion of the orthometallated *p*-tolyl group of **6t**, through a similar 1,3-hydrogem migration leading to **6t'$_3$**, was also calculated for comparative purpose. The results nicely agree with the previous findings (Scheme 6). Dearomatization of both iridafuran rings of **3t** produces a loss of stability, being greater for the dearomatization of the ring with the metallated carbon atom located *trans* to the chloride ligand (21.7 *versus* 18.2 kcal mol^{-1}); the counterpart of that of **3** with higher negative NICS values. The isomerization in **6t** produces similar effects. Consistent with NICS values of **6**, the dearomatization of the ring with the metallated carbon atom *trans* to the pyridyl group gives rise to a higher loss of stability than the dearomatization of the ring with the carbon atom t*rans* to the *p*-tolyl group (26.6 *versus* 21.4 kcal

mol^{-1}). The loss of stability by dearomatization of the iridafuran rings of both complexes, **3t** and **6t**, is lower than that produced by a similar isomerization in the orthometallated *p*-tolyl moiety of the *C,N*-chelate (34.4 kcal mol^{-1}).

Scheme 6. Aromaticity of Rings of Model Complexes 3t and 6t Evaluated by the Aromatic Stabilization Energy (ASE; kcal mol^{-1}) Method

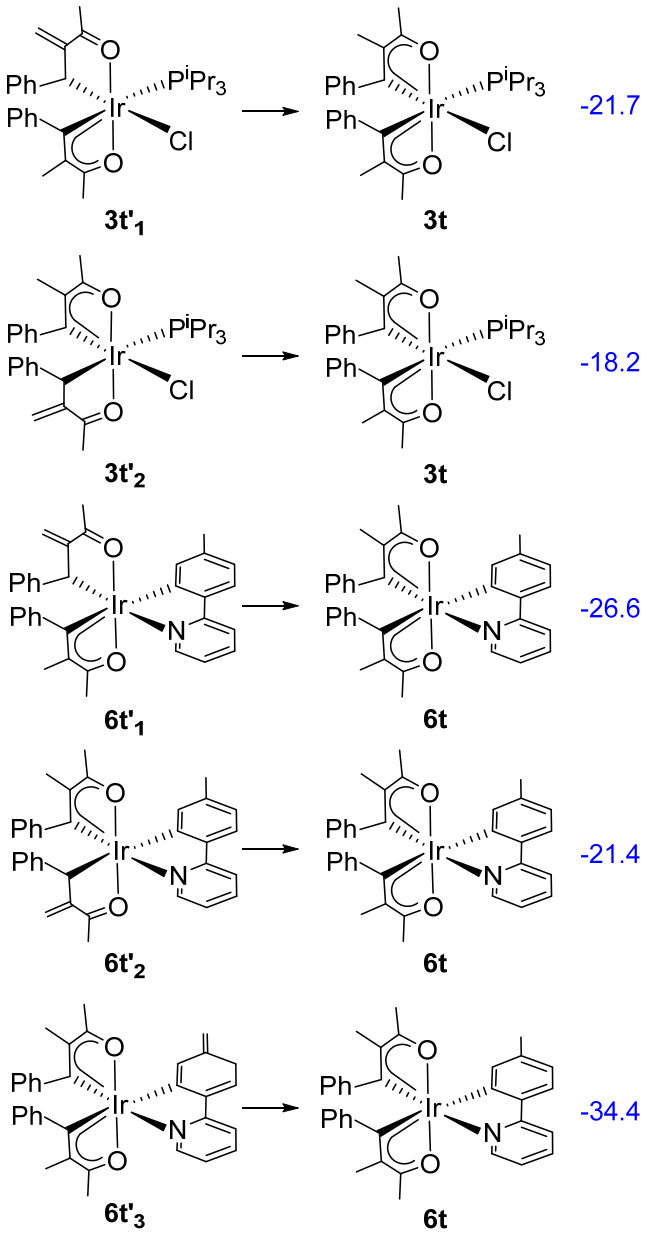

Bromination Reactions. Molecular bromine is a common reagent in bromination reactions,[30] but its use has several disadvantages; it is dangerous and very irritating, whereas the reactions are rarely selective. Among the alternatives, *N*-bromosuccinimide (NBS) occupies a distinguished position, due to its accessibility, easy handling and stability.[31] It is particularly useful for the metal-catalyzed *meta*-selective C-H bromination of aryl groups, when attached to a heterocyclic assistant.[32] We have previously used it to construct heteroleptic iridium(III) phosphorescent emitters by selective post-functionalization of homoleptic precursors.[33] Its success in this synthetic methodology inspired us to now apply it in the confirmation of the aromatic nature of the spiro iridafurans derivatives discovered.

Bromination is sensitive to the degree of aromaticity of the iridafuran ring, which is tuned by the ligand located in *trans* to the metallated carbon atom. Therefore, it is directed by said ligand. This is strongly supported by the behavior of **3**, which arranges the metallated carbon atoms of the spiro iridafurans *trans* to electronically very different ligands (Scheme 7). Indeed, the addition of 1.0 equiv of NBS to the solutions of **3**, in dichloromethane, at room temperature gives rise to the instantaneous and selective C-H functionalization of the iridafuran ring that has the metallated carbon atom *trans* to the chloride ligand (**b$_1$** in Charts 2-4). It should be noted that it is the spiro unit ring that shows the most negative NICS values and possesses the most negative CH-carbon atom. Bromination yields IrCl{κ^2-*C,O*-[C(Ph)CBrC(Me)O]}{κ^2-*C,O*-[C(Ph)CHC(Me)O]}(P^{i}Pr$_3$) (**8**), which was isolated as an orange solid in 86% yield and characterized by X-ray diffraction analysis. The structure[29] (Figure 4) is consistent with the selectivity of the electrophilic hydrogen substitution and the chloride *trans*-control on the bromination. The selectivity is also supported by the ^{1}H NMR spectrum of the orange solid, in dichloromethane-d_2, at room temperature, which shows only one resonance at 6.68 ppm from the two observed in the region between 6.5 and 7.0

ppm, in the spectrum of **3**. This signal corresponds to the hydrogen atom of the not attacked ring. A noticeable electronic change resulting from the reaction is the decrease in absolute value of the negative NBO charge on the brominated carbon atom with respect to the charge of the hydrogenated carbon (-0.290 *versus* -0.438), which practically maintains that of **3.** Consistently with this fact, the addition of a second equiv of NBS to the solutions of **8**, in dichloromethane, at room temperature leads to IrCl{κ^2-*C,O*-[C(Ph)CBrC(Me)O]}$_2$(P^{i}Pr$_3$) (**9**), as a result from the C-H functionalization of the other iridafuran ring; that containing the metallated carbon atom disposed *trans* to the phosphine. This dibrominated species was also isolated as an orange solid in 86% yield and characterized by X-ray analysis. Figure 5 gives a view of the octahedral structure of the molecule. In accordance with a second bromination, the ^{1}H NMR spectrum of **9** does not contain any characteristic resonance for a CH-hydrogen atom of iridafuran.

Scheme 7. Bromination of Complex 3 (NBO charges in blue)

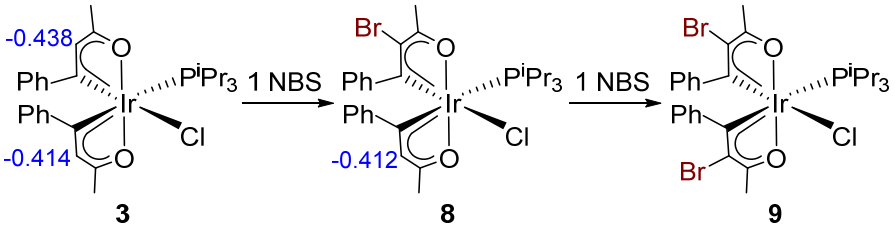

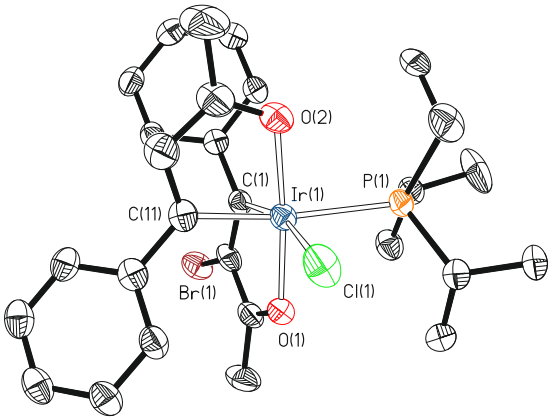

Figure 4. Molecular diagram of one of the two chemically equivalent but crystallographically independent molecules of complex **8** (displacement ellipsoids shown at 50% probability). All hydrogen atoms are omitted for clarity. Selected bond distances (Å) and angles (deg): Ir(1)-P(1) = 2.4349(12), 2.4289(12), Ir(1)-Cl(1) = 2.4479(13), 2.4567(10), Ir(1)-O(1) = 2.030(3), 2.046(3), Ir(1)-O(2) = 2.038(4), 2.033(3), Ir(1)-C(1) = 1.986(5), 1.983(4), Ir(1)-C(11) = 2.042(5), 2.059(4); C(1)-Ir(1)-O(1) = 80.91(17), 80.71(16), C(11)-Ir(1)-O(2) = 78.93(18), 79.74(15), O(1)-Ir(1)-O(2) = 174.94(15), 175.58(13), C(11)-Ir(1)-P(1) = 169.44(14), 166.79(13), C(1)-Ir(1)-Cl(1) = 164.93(13), 168.69(13).

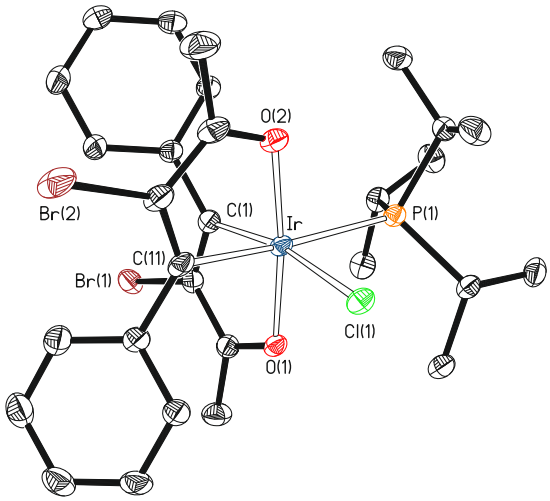

Figure 5. Molecular diagram of complex **9** (displacement ellipsoids shown at 50% probability). All hydrogen atoms are omitted for clarity. Selected bond distances (Å) and angles (deg): Ir-P(1) = 2.4105(7), Ir-Cl(1) = 2.4484(7), Ir-O(1) = 2.0304(19), Ir-O(2) = 2.041(2), Ir-C(1) = 1.994(3), Ir-C(11) = 2.061(3); C(1)-Ir-O(1) = 80.42(10), C(11)-Ir-O(2) = 79.55(10), O(1)-Ir-O(2) = 173.55(8), C(11)-Ir-P(1) = 173.03(9), C(1)-Ir-Cl(1) = 168.43(8).

The complex **6** with an orthometallated 2-*p*-totylpyridine arranged *trans* to the metallated carbon atoms of the spiro iridafurans shows selectivity consistent with that of **3**. Its reaction with 1.0 equiv of NBS, in dichloromethane, at room temperature gives Ir{κ^2-*C,O*-[C(Ph)CBrC(Me)O]}{κ^2-*C,O*-[C(Ph)CHC(Me)O]}{κ^2-*C,N*-[C$_6$MeH$_3$-py]} (**10**), resulting from the exclusive substitution of hydrogen by bromine in the iridafuran with the metallated carbon atom *trans* to the pyridyl group; the spiro unit ring showing the most negative NICS values and the CH-carbon atom having the slightly higher negative NBO charge (-0.428 *versus* -0.424). Complex **10** was isolated as a red solid in 89% yield (Scheme 8). Like **8** and **9**, it was characterized by X-ray diffraction analysis. The structure (Figure 6) is consistent with the selectivity of electrophilic substitution and the tris(heteroleptic) nature of the complex containing three different 3e donor bidentate ligands. Consistent with the reaction, the ^{1}H NMR spectrum of the isolated solid, in dichloromethane-*d*$_2$, at room temperature contains only one signal that can be assigned to a CH-hydrogen atom of iridafuran, at 7.14 ppm.

Scheme 8. Bromination of Complex 6 (NBO charges in blue)

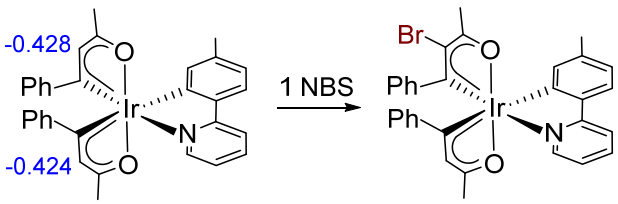

6 **10**

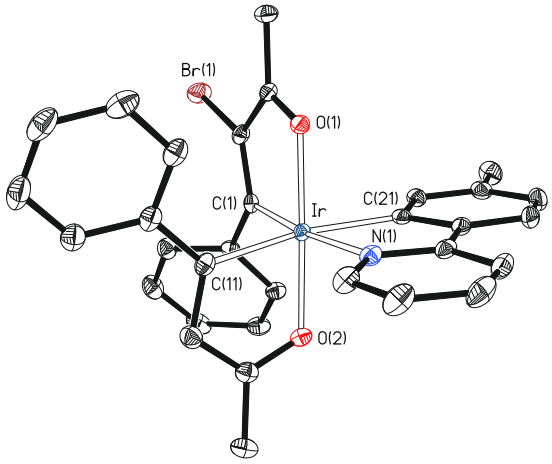

Figure 6. Molecular diagram of complex **10** (displacement ellipsoids shown at 50% probability). All hydrogen atoms are omitted for clarity. Selected bond distances (Å) and angles (deg): Ir-O(1) = 2.0281(16), Ir-O(2) = 2.0411(17), Ir-C(1) = 1.972(2), Ir-C(11) = 2.076(2), Ir-N(1) = 2.134(2), Ir-C(21) = 2.076(2); O(1)-Ir-C(1) = 80.56(8), O(2)-Ir-C(11) = 78.82(8), N(1)-Ir-C(21) = 78.31(9), O(1)-Ir-O(2) = 176.99(6), C(1)-Ir-N(1) = 173.42(9), C(11)-Ir-C(21) = 170.09(9).

The formation of **8** and **10** follows the same pattern; in both cases the C-H functionalization takes place in the most aromatic five-membered ring and the attack occurs on the carbon atom with the greatest negative NBO charge. To understand why this happens, we analyzed the thermodynamics and kinetics of the bromination of **6** by DFT calculations at the SMD(dichloromethane)-B3LYP-D3//SDD(f)-6-31G** level with dispersion correction (see computational details in the Supporting Information file). The attack on both iridafurans was studied separately. The free energy variations (ΔG) were calculated at 298.15 K and 1 atm. Figure 7 shows the calculated reaction profile for the bromination of the iridafuran with the metallated carbon atom *trans* to the pyridyl group, the bromination experimentally observed, whereas Figure S28 gives the profile for the bromination of the other iridafuran. As expected, the substitutions are

thermodynamically favored, with the stability of both isomers being similar (≈ -28 kcal mol^{-1}). The bromination mechanism is typical of an electrophilic aromatic substitution with the stages usually proposed.[21g,34] The rate determined step is the NBS attack on the CH-carbon atom. The attack that leads to the experimentally observed bromination is favored kinetically (16.6 *versus* 20.1 kcal mol^{-1}). Therefore, the selectivity is of kinetic origin. The activation energy seems to depend on the NBO charge of the carbon atom, the lowest corresponding to the attack on the carbon that bears the most negative charge.

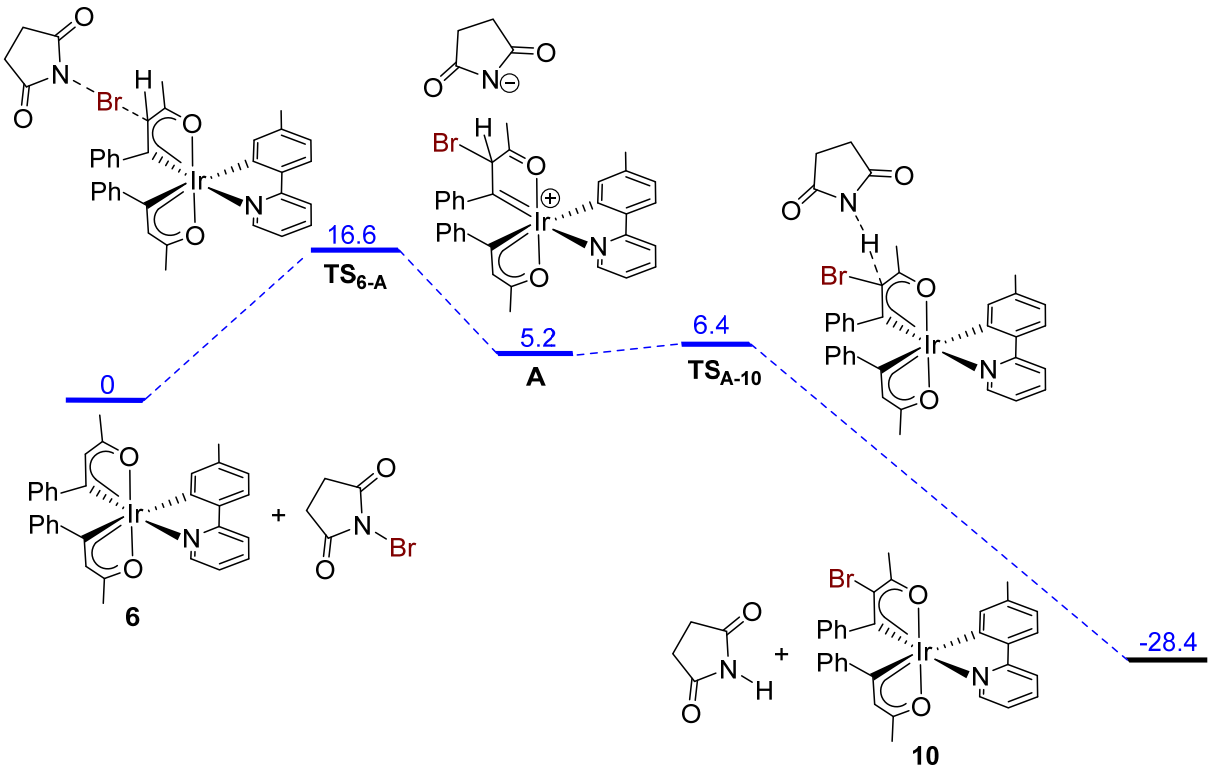

Figure 7. Computed energy profile (SMD(dichloromethane)-B3LYP-D3//SDD(f)-6-31G** level) for the bromination of complex **6** to give **10**. The relative 298 K Gibbs free energies in dichloromethane are given in kcal mol^{-1}.

We note that previously the orthometallated *p*-tolyl groups of the dimer [Ir(μ-Cl){κ^2-*C,N*-(C_6H_3Me-py)}$_2$]$_2$ have also been selectively brominated, in *para* position with respect to the Ir-C bond, with NBS.[33] To gain insight into why the bromination of the orthometallated *p*-tolyl group is not observed in this case, we also studied the bromination of such moiety. Figure S29 shows the reaction profile. The results reinforce the idea that the selectivity of these bromination reactions is of kinetic origin and that the activation energy of the electrophilic substitution is a function of the negative charge on the attacked carbon atom. Consistent with this, the bromination of the *p*-tolyl group is an exothermic reaction at the same amount of energy as the previous brominations, around -28 kcal mol^{-1}. However, its activation energy is significantly higher than in the previous cases, 28.3 kcal mol^{-1}, as corresponds to a lower negative NBO charge on the attacked carbon atom (-0.258 *versus* -0.424 and -0.428).

The reaction of complex **7** with NBS provides conclusive evidence of the relevance of the NBO charge in directing the attack of the brominating agent (Scheme 9). The C^3 atom of the acac ligand of this species carries an NBO charge of -0.512. This charge is significantly more negative than that of the CH-carbon atoms of the iridafuran rings, -0.430. The C^3 carbon of the acac ligand is precisely the atom attacked in this case. Treatment of solutions of **7**, in dichloromethane, with 1.0 equiv of NBS, at room temperature, for 1 h leads selectively to Ir{κ^2-*C,O*-[C(Ph)CHC(Me)O]}$_2${κ^2-*O,O*-[acacBr]} (**11**), as a result of the replacement of the hydrogen atom at the C^3-carbon of acac by bromine. Complex **11** was isolated as a red solid in 78% yield and characterized by X-ray diffraction analysis. The structure (Figure 8) demonstrates the bromination of the acac ligand. In agreement with this, the ^{1}H NMR spectrum of the red solid, in dichloromethane-d_2, at room temperature does not contain any signal that can be assigned to the

characteristic C^3H-hydrogen atom, while it shows a resonance due to the CH-hydrogen atom of the iridafuran rings, at 6.75 ppm.

Scheme 9. Bromination of Complex 7 (NBO charges in blue)

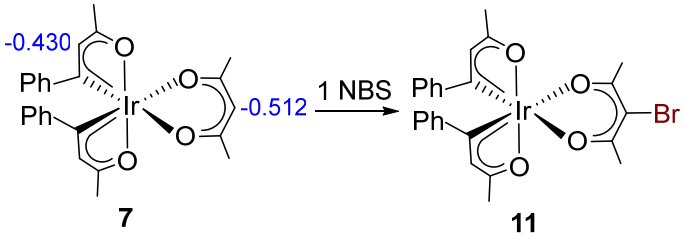

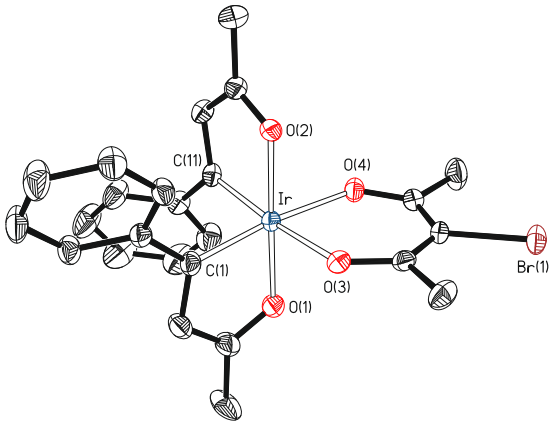

Figure 8. Molecular diagram of complex **11** (displacement ellipsoids shown at 50% probability). All hydrogen atoms are omitted for clarity. Selected bond distances (Å) and angles (deg): Ir-O(1) = 2.0357(15), Ir-O(2) = 2.0314(14), Ir-O(3) = 2.1149(15), Ir-O(4) = 2.1196(14), Ir-C(1) = 1.979(2), Ir-C(11) = 1.971(2); O(1)-Ir-C(1) = 80.59(7), O(2)-Ir-C(11) = 80.23(7), O(3)-Ir-O(4) = 85.62(6), O(1)-Ir-O(2) = 178.36(6), C(1)-Ir-O(4) = 172.31(7), C(11)-Ir-O(3) = 171.36(7) .

Structural criteria (Chart S1) and AICD computational results (Figures S35-S38) as well as NICS scans (Figures S44-S47 and Table 1) also indicate the aromatic character of spiro iridafurans **8-11**.

CONCLUSION

This study reveals the existence of spiro iridafurans molecules and cations, which carry orthogonally arranged five-membered rings and the oxygen atoms located in mutually *trans* positions, in an octahedral environment of the iridium atom. They result from the $C_{\beta}(sp^2)$-H bond activation of two molecules of benzylideneacetone on an iridium center. The spiro iridafurans moiety is aromatic, according to the structural criterion. The aromaticity has been also supported by computational methods, including AICD, NICS, ASE, and NBO analysis, and experimentally confirmed by bromination of the iridafuran rings, with NBS, through electrophilic hydrogen substitution.

The bonding situation in five-membered rings is the result of an asymmetric contribution of two resonance forms, namely: alkylidene (f_1) and alkenyl (f_2). The system increases the aromatic character when the respective contributions are close. The contribution of each one to a particular ring depends on the ligand or group arranged *trans* to the carbon atom directly attached to the metal center. Therefore, the degree of aromaticity of the spiro iridafuran rings is governed by said ligands or groups. Such ligand or group also determines the negative charge of the CH-carbon atom.

Bromination reactions are sensitive to both the degree of aromaticity of the ring and the negative charge of the attacked CH-carbon atom. Thus, they are also governed by the ligand or group arranged *trans* to the carbon atom directly attached to the metal. As a consequence, the five-membered rings can be selectively brominated, when different ligands or groups lie *trans* to these metallated atoms. The origin of the selectivity is kinetic. The bromination mechanism is typical of an electrophilic aromatic substitution, the rate-determining step of the reaction being the attack of

the brominating agent on the CH-carbon atom. The activation energy depends on the negative charge of this atom; a higher negative charge allows for a lower activation energy.

Spiro metallaromatic compounds were hitherto a few lithium-stabilized spiro metallahydrocarbons derivatives. This class of complexes has new members. They are a family of aromatic spiro iridafurans, which do not require external stabilization. The discovery of these compounds augurs a rapid development of spiro metallaheterocycles, given the great conceptual interest of spiro metallaromatic compounds and the possibilities offered by transition metals to stabilize spiro aromatic structures.

EXPERIMENTAL SECTION

General Information. All reactions were carried out with exclusion of air using Schlenk-tube techniques or in a drybox. Instrumental methods and X-ray details are given in the Supporting Information. The NMR spectra (Figures S1-S26) were recorded at 298 K and the chemical shifts (in ppm) are referenced to residual solvent peaks (^{1}H, ^{13}C{^{1}H}) or external 85% H_3PO_4 (^{31}P{^{1}H}), while coupling constants *J* are given in hertz. [Ir(μ-Cl)(C_8H_{14})$_2$]$_2$ (**1**) was prepared according to the reported procedure.[35]

Preparation of [Ir(μ-Cl){κ^2-*C,O*-[C(Ph)CHC(Me)O]}$_2$]$_2$ (2). To 100 mg of **1** (0.11 mmol) in a Schlenk flask were added 160 mg of benzylideneacetone (1.1 mmol). The mixture was heated at 100 °C, at which the ketone melted, for 2 h and the mixture became dark red. After 2 additional hours the mixture was cooled down to room temperature, 20 mL of Et_2O were added and an intense red precipitate formed. The supernatant was removed and the solid washed with Et_2O (3 x 20 mL) and dried *in vacuo* (92 mg, 79%). ^{1}H NMR (400 MHz, CD_2Cl_2): δ 7.37-7.25 (overlapping signals, 20H, Ph), 6.54 (s, 4H, IrC-C-H), 2.47 (s, 12H, CH_3). ^{13}C{^{1}H} NMR (100.6 MHz, CD_2Cl_2): δ 217.4

(s, Ir-C), 205.7 (s, C-O), 145.3 (s, C_q Ph), 133.8 (s, IrC-*C*-H), 129.3, 128.2, 126.2 (all s, CH Ph), 23.7 (s, CH_3). HRMS (electrospray, *m/z*) calcd. for $C_{40}H_{36}Cl_2Ir_2NaO_4$ $[M + Na]^+$: 1059.1121; found: 1059.1133. Anal. calcd. for $C_{40}H_{36}Cl_2Ir_2O_4$ (%): C, 46.37; H, 3.50. Found: C, 45.98; H, 3.86. IR (cm^{-1}): ν(C=O) 1655, ν(C=C) 1538.

Isomerization of 2 into 2a. A solution of **2** (10 mg, 0.01 mmol) in toluene-d_8 was heated at 100 °C for 16 hours in an NMR tube. After this time, ^1H and $^{13}C\{^1H\}$ NMR spectra were recorded and a mixture 1:1 of **2** and **2a** was observed. In toluene-d_8, the characteristic ring CH signal of **2** is observed at 6.31 ppm, while the corresponding CH signal for **2a** is observed at 6.34 ppm. Regarding $^{13}C\{^1H\}$, the C-Ir signals in toluene-d_8 appear at 216.4 for **2** and 216.5 for **2a**, while the C-O signals appear a 205.5 and 206.1 for **2** and **2a**, respectively.

Preparation of IrCl{κ²-*C,O*-[C(Ph)CHC(Me)O]}(P^iPr_3) (3). To a stirred solution of **2** (100 mg, 0.096 mmol) in dichloromethane (5 mL) was added dropwise P^iPr_3 (46 μL, 0.24 mmol). The reaction was stirred for 2 h after which the solvent was removed *in vacuo*. The resulting orange solid was washed with pentane (3 x 5 mL) and dried *in vacuo* to obtain **3** as an orange powder (110 mg, 84%). ^1H NMR (400 MHz, CD_2Cl_2): δ 7.34-7.17 (overlapping signals, 10H, CH Ph), 6.73 (s, 1H, IrC-C-H), 6.57 (d, $^3J_{H-P}$ = 8.1, 1H, IrC-C-H), 2.92-2.79 (m, 3H, C*H*$(CH_3)_2$), 2.44 (s, 3H, CH_3), 2.17 (d, $^5J_{H-P}$ = 2.1, 3H, CH_3), 1.26 (dd, $^3J_{H-P}$ = 13.5, $^3J_{H-H}$ = 7.2, 9H, CH(C*H*$_3$)), 1.18 (dd, $^3J_{H-P}$ = 13.5, $^3J_{H-H}$ = 7.2, 9H, CH(C*H*$_3$)$_2$). $^{13}C\{^1H\}$ NMR (100.6 MHz, CD_2Cl_2): δ 224.4 (d, $^2J_{C-P}$ = 87, C-Ir), 218.4 (d, $^2J_{C-P}$ = 9, C-Ir), 212.8 (s, C-O), 210.8 (s, C-O), 146.3 (C_q Ph), 143.3 (d, $^3J_{C-P}$ = 2, C_q Ph), 132.5 (d, $^3J_{C-P}$ = 2, IrC-*C*-H), 132.4 (s, IrC-*C*-H), 129.7, 128.6, 128.1, 127.9, 127.8 (all s, CH Ph), 126.6 (d, $^4J_{C-P}$ = 2, CH Ph), 24.6 (s, CH_3), 24.1 (d, $^1J_{C-P}$ = 20, *C*H$(CH_3)_2$), 22.7 (s, CH_3), 19.5 (s, CH(*C*H$_3$)$_2$), 19.3 (d, $^2J_{C-P}$ = 2, CH(*C*H$_3$)$_2$). $^{31}P\{^1H\}$ NMR (161.9 MHz, CD_2Cl_2): δ 3.5 (s). HRMS (electrospray, *m/z*) calcd. for $C_{29}H_{39}IrO_2P$ $[M - Cl]^+$: 643.2313; found: 643.2395. Anal.

calcd. for $C_{29}H_{39}ClIrO_2P$ (%): C, 51.35; H, 5.80. Found: C, 51.21; H, 5.74. IR (cm^{-1}): ν(C=O) 1544, ν(C=C) 1514.

Preparation of [Ir{κ²-*C,O*-[C(Ph)CHC(Me)O]}₂(MeCN)₂]BF_4 (4). To a stirred solution of **2** (112 mg, 0.1 mmol) in MeCN (5 mL) was added in one portion $AgBF_4$ (42 mg, 0.2 mmol). The reaction mixture was stirred for 2 h protected from the light, after which the solvent was removed *in vacuo*, the mixture dissolved in dichloromethane and filtered through a pad of Celite. The resulting yellow solution was concentrated *in vacuo* and addition of Et_2O (10 mL) produced the precipitation of an intense yellow solid, which was washed with Et_2O (3 x 5 mL). The resulting solid was dried *in vacuo* to obtain **4** as a yellow powder (121 mg, 86%). ^1H NMR (400 MHz, CD_2Cl_2): δ 7.48-7.38 (overlapping signals, 6H, CH Ph), 7.28-7.26 (overlapping signals, 4H, CH Ph), 6.62 (s, 2H, IrC-C-H), 2.65 (s, 6H, Ir-NCMe), 2.43 (s, 6H, CH_3). $^{13}C\{^1H\}$ NMR (100.6 MHz, CD_2Cl_2): δ 219.4 (s, C-Ir), 204.8 (C-O), 142.5 (s, C_q Ar), 133.8 (s, IrC-*C*-H), 130.2, 127.9, 126.5 (all s, CH Ph), 23.6 (s, CH_3), 3.5 (s, IrMeCN). $^{19}F\{^1H\}$ NMR (376.5 MHz, CD_2Cl_2): δ -152.7 (s, BF_4). HRMS (electrospray, *m/z*) calcd. for $C_{24}H_{24}IrN_2O_2$ $[M]^+$: 565.1462; found: 565.1441. Anal. calcd for $C_{24}H_{24}BF_4IrN_2O_2$ (%): C, 44.25; H, 3.71. Found: C, 44.29; H, 3.72. IR (cm^{-1}): ν(C=O) 1537, ν(C=C) 1408.

Preparation of [Ir(μ-OH){κ²-*C,O*-[C(Ph)CHC(Me)O]}₂]₂ (5). To a solution of **2** (112 mg, 0.11 mmol), in acetone (5 mL), at room temperature was added in one portion aqueous KOH (0.5 M, 0.5 mL, 0.25 mmol) and stirred for 30 min. The mixture was evaporated to dryness The residue extracted with dichloromethane and the suspension was filtered through a plug of Celite, The resulting solution was evaporated to afford a red/purple solid, which was washed with Et_2O (3 x 5 mL), and dried *in vacuo* (95 mg, 88%). ^1H NMR (400 MHz, CD_2Cl_2): δ 7.29-7.10 (overlapping signals, 20H, Ph), 6.87 (s, 4H, IrC-C-H), 2.51 (s, 12H, CH_3), 0.27 (s, 2H, OH). $^{13}C\{^1H\}$ NMR

(100.6 MHz, CD_2Cl_2): δ 214.9 (s, Ir-C), 214.4 (s, C-O), 148.5 (s, C_q Ph), 134.5 (s, IrC-*C*-H), 129.2, 128.3, 126.2 (all s, CH Ph), 23.7 (s, CH_3). HRMS (electrospray, *m/z*) calcd for $C_{20}H_{20}IrNaO_3$ $[M/2+H+Na]^+$: 524.0934; found: 524.0917. Anal. calcd. for $C_{40}H_{38}Ir_2O_6$ (%): C, 48.08; H, 3.83. Found: C, 48.43; H, 4.14. IR (cm^{-1}): ν(O-H) 3569, (C=C) 1643.

Preparation of Ir{κ²-*C,O*-[C(Ph)CHC(Me)O]}₂{κ²-*C,N*-[C_6MeH_3-py]} (6). To a stirred solution of **4** (100 mg, 0.15 mmol) in fluorobenzene (5 mL) was added in one portion 2-(*p*-tolyl)pyridine (26 μL, 0.15 mmol) and (piperidinomethyl)polystyrene (88 mg, 2 eq). The reaction mixture was refluxed for 12 hours, after which the solvent was removed *in vacuo,* dissolved in dichloromethane and filtered through a pad of Celite. The resulting red solution was dried *in vacuo* and the solid washed with Et_2O (3 x 5 mL). The resulting red solid was dried *in vacuo* to obtain **6** as a red powder (83 mg, 83%). ^1H NMR (400 MHz, CD_2Cl_2): δ 8.32 (d, $^3J_{H-H}$ = 5.4, 1H, CH Ar), 7.95 (d, $^3J_{H-H}$ = 8.2, 1H, CH Ar), 7.74-7.70 (overlapping signals, 2H, CH Ar), 7.39-7.26 (overlapping signals, 10H, CH Ar), 7.16 (s, 1H, IrC-C-H), 7.14 (s, 1H, CH Ar), 7.03 (m, 1H, CH Ar), 6.91 (s, 1H, IrC-C-H), 6.88 (dd, $^3J_{H-H}$ = 7.9, $^4J_{H-H}$ = 1.4, 1H, CH Ar), 2.26 (s, CH_3), 2.24 (s, CH_3), 2.19 (s, CH_3). $^{13}C\{^1H\}$ NMR (100.6 MHz, CD_2Cl_2): δ 238.9 (s, C-Ir), 218.9 (s, C-Ir), 217.3 (s, C-O), 209.8 (C-O), 168.5 (s, C_q Ar), 168.3 (s, C_q Ar), 153.8 (s, CH Ar), 147.7 (s, C_q Ar), 147.1 (s, C_q Ar), 144.2 (C_q-Ir), 141.7, 140.4, 137.9 (all s, CH Ar), 132.8 (IrC-*C*-H), 130.0 (IrC-*C*-H), 129.4, 128.8, 128.5, 128.1, 127.7, 127.3, 124.1, 122.6 (all s, CH Ar), 118.9 (C_q Ar), 24.1, 22.9, 21.8 (all s, CH_3). HRMS (electrospray, *m/z*) calcd. for $C_{32}H_{29}IrNO_2$ $[M+H]^+$: 652.1824; found. 652.1808. Anal. calcd for $C_{32}H_{28}IrNO_2$ (%); C, 59.06; H, 4.34; N, 2.15. Found: C, 58.97; H, 4.38; N, 2.05. IR (cm^{-1}): ν(C=O) 1584, ν(C=C) 1505.

Preparation of Ir{κ²-*C,O*-[C(Ph)CHC(Me)O]}₂{κ²-*O,O*-[acac]} (7). *Method a:* Acetylacetone (51 μL, 0.5 mmol) was added to a purple red suspension of **5** (100 mg, 0.1 mmol)

in acetone (5 mL) and the mixture was stirred at 50 ºC for 24 hours. After this time, the solvent was removed under vacuum and the addition of pentane (4 mL) led to a red solid, which was washed with pentane (3 x 3 mL) and dried under vacuum (112 mg, 96%). *Method b:* To a stirred solution of **2** (135 mg, 0.1 mmol) in dichloromethane (3 mL) was added in one portion sodium acetylacetonate (25 mg, 0.2 mmol). The reaction was stirred for 1 h after which the reaction was filtered through a pad of Celite, and the solvent was removed in vacuo. The resulting red residue was washed with Et_2O (5 x 5 mL) and the residue dried *in vacuo* to give **7** as red solid (111 mg, 75%). ^{1}H NMR (400 MHz, CD_2Cl_2): δ 7.31-7.19 (overlapping signals, 10H, Ph), 6.77 (s, 2H, IrC-C-H), 5.44 (s, 1H, CH acac), 2.42 (s, 6H, CH_3), 2.01 (s, 6H, CH_3). ^{13}C{^{1}H} NMR (100.6 MHz, CD_2Cl_2): δ 216.5 (s, Ir-C), 211.7 (s, C-O), 186.3 (s, C-O acac), 147.1 (s, C Ph), 134.7 (s, IrC-C-H), 129.6, 128.3, 126.5 (all s, CH Ph), 100.9 (s, CH acac), 28.4 (s, CH_3), 23.6 (s, CH_3). HRMS (electrospray, *m/z*) calcd. for $C_{25}H_{26}IrO_4$ $[M+H]^+$: 583.1456; found: 583.1431. Anal. calcd for $C_{25}H_{25}IrO_4$ (%): C, 51.62; H, 4.33. Found: C, 51.23; H, 4.28. IR (cm^{-1}): ν(C=O) 1578, ν(C=C) 1509.

Preparation of IrCl{κ^2-*C,O*-[C(Ph)CBrC(Me)O]}{κ^2-*C,O*-[C(Ph)CHC(Me)O]}(P^{i}Pr$_3$) (8). To a stirred solution of **3** (67.8 mg, 0.1 mmol), in dichloromethane (5 mL), at room temperature was added dropwise a solution of *N*-bromosuccinimide (17.8 mg, 0.1 mmol) in dichloromethane (1 mL). The reaction was stirred for 5 min protected from the light and then the solvent was removed *in vacuo*. The resulting orange solid was washed with Et_2O (3 x 5 mL) and pentane (3 x 5 mL) and dried *in vacuo* to obtain **8** as an orange powder (65 mg, 86%). ^{1}H NMR (400 MHz, CD_2Cl_2): δ 7.33-7.29 (overlapping signals, 8H, CH Ph), 7.05-7.03 (overlapping signals, 2H, CH Ph), 6.68 (d, $^4J_{H\text{-}P}$ = 8.3, IrC-C-H), 2.85 (m, 3H, C*H*$(CH_3)_2$), 2.36 (s, CH_3), 2.32 (d, $^5J_{H\text{-}P}$ = 2.2, CH_3), 1.25-1.16 (overlapping signals, 18H, $CH(CH_3)_2$). ^{13}C{^{1}H} NMR (100.6 MHz, CD_2Cl_2): δ

223.0 (d, $^{2}J_{C\text{-}P}$ = 87, C-Ir), 219.3 (d, $^{2}J_{C\text{-}P}$ = 9, C-Ir), 211.5 (d, $^{3}J_{C\text{-}P}$ = 3, C-O), 204.5 (d, $^{3}J_{C\text{-}P}$ = 3, C-O), 146.0 (s, C_q Ph), 142.8 (s, C_q Ph), 132.8 (s, IrC-C-H), 128.8, 128.3, 128.0, 127.8, 126.5, 126.4 (all s, CH Ph), 113.6 (s, C-Br), 24.9 (s, CH_3), 24.5 (s, CH_3), 24.4 (d, $^{1}J_{C\text{-}P}$ = 20, *C*H(CH_3)$_2$), 19.3 (s, CH(*C*H_3)$_2$), 18.9 (d, $^{2}J_{C\text{-}P}$ = 2, CH(*C*H_3)$_2$. $^{31}P\{^{1}H\}$ NMR (161.9 MHz, CD_2Cl_2): δ 2.7 (s). HRMS (electrospray, *m/z*) calcd. for $C_{29}H_{38}BrIrO_2P$ $[M - Cl]^+$: 721.1402; found: 721.1393. Anal. calcd. for $C_{29}H_{38}BrClIrO_2P$ (%): C, 46.00; H, 4.95. Found: C, 46.28; H, 4.98. IR (cm^{-1}): ν(C=O) 1694, ν(C=C) 1544.

Preparation of IrCl{κ²-*C,O*-[C(Ph)CBrC(Me)O]}$_2$(P^{i}Pr$_3$) (9). To a stirred solution of **3** (67.8 mg, 0.1 mmol), in dichloromethane (5 mL), at room temperature was added dropwise a solution of *N*-bromosuccinimide (35.6 mg, 0.2 mmol) in dichloromethane (1 mL). The reaction was stirred for 5 min protected from the light and then the solvent was removed *in vacuo*. The resulting orange solid was washed with Et_2O (3 x 5 mL) and pentane (3 x 5 mL) and dried *in vacuo* to obtain **9** as an orange powder (72 mg, 86%). ^{1}H NMR (400 MHz, CD_2Cl_2): δ 7.37-7.30 (overlapping signals, 6H, CH Ph), 7.15-7.11 (overlapping signals, 2H, CH Ph), 7.02-6.99 (overlapping signals, 2H, CH Ph), 2.88-2.76 (m, 3H, C*H*(CH_3)$_2$), 2.61 (s, 3H, CH_3), 2.10 (d, $^{5}J_{H\text{-}P}$ = 1.9, CH_3), 1.14 (dd, $^{3}J_{H\text{-}P}$ = 13.3, $^{3}J_{H\text{-}H}$ = 7.4, 18H, CH(C*H*$_3$)$_2$). $^{13}C\{^{1}H\}$ NMR (100.6 MHz, CD_2Cl_2): δ 217.6 (d, $^{2}J_{C\text{-}P}$ = 9, C-Ir), 214.6 (d, $^{2}J_{C\text{-}P}$ = 86, C-Ir), 213.1 (d, $^{3}J_{C\text{-}P}$ = 3, C-O), 202.2 (d, $^{3}J_{C\text{-}P}$ = 3, C-O), 146.4 (s, C_q Ph), 141.6 (s, C_q Ph), 128.6, 128.2, 127.9, 127.5, 125.8, 124.8 (all s, CH Ph), 114.7 (d, $^{3}J_{C\text{-}P}$ = 4, C-Br), 114.6 (s, C-Br), 26.9 (s, CH_3), 24.9 (d, $^{1}J_{C\text{-}P}$ = 22, *C*H(CH_3)$_2$), 24.6 (s, CH_3), 19.1 (s, CH(*C*H_3)$_2$), 18.7 (d, $^{2}J_{C\text{-}P}$ = 2, CH(*C*H_3)$_2$). $^{31}P\{^{1}H\}$ NMR (161.9 MHz, CD_2Cl_2): δ 1.1 (s). HRMS (electrospray, *m/z*) calcd. for $C_{29}H_{37}Br_2IrClNaO_2P$ $[M + Na]^+$: 859.0075; found: 859.0047. Anal. calcd. for $C_{29}H_{37}Br_2ClIrO_2P$ (%): C, 41.66; H, 4.46. Found: C, 41.37; H, 4.38. IR (cm^{-1}): ν(C=O) 1695, ν(C=C) 1541.

Preparation of Ir{κ²-*C,O*-[C(Ph)CBrC(Me)O]}{κ²-*C,O*-[C(Ph)CHC(Me)O]}{κ²-*C,N*-[C_6MeH_3-py]} (10). To a stirred solution of **6** (65 mg, 0.1 mmol), in dichloromethane (3 mL), at room temperature was added dropwise a solution of *N*-bromosuccinimide (17.8 mg, 0.1 mmol) in dichloromethane (1 mL). The reaction was stirred for 5 min protected from the light and then the solvent was removed *in vacuo*. The resulting red solid was washed with Et_2O (3 x 5 mL) and pentane (3 x 5 mL) and dried *in vacuo* to obtain **10** as a red powder (65 mg, 89%). ^{1}H NMR (400 MHz, CD_2Cl_2): δ 8.29 (d, $^3J_{H-H}$ = 5.6, 1H, CH Ar), 7.93 (d, $^3J_{H-H}$ = 8.2, 1H, CH Ar), 7.73-7.69 (overlapping signals, 2H, CH Ar), 7.42-7.34 (overlapping signals, 6H, CH Ar), 7.29-7.23 (overlapping signals, 4H, CH Ar), 7.18-7.16 (m, 1H, CH Ar), 7.14 (s, 1H, IrC-C-H), 7.00 (ddd, $^3J_{H-H}$ = 7.2, $^3J_{H-H}$ = 5.6, $^4J_{H-H}$ = 1.4, 1H, CH Ar), 6.92 (d, $^3J_{H-H}$ = 7.8, 1H, CH Ar). 2.43 (s, CH_3), 2.33 (s, CH_3), 2.00 (s, CH_3). ^{13}C{^{1}H} NMR (100.6 MHz, CD_2Cl_2): δ 237.3 (s, C-Ir), 218.2 (s, C-Ir), 213.2 (s, C-O), 207.5 (C-O), 168.5 (s, C_q Ar), 167.5 (s, C_q Ar), 153.9 (s, CH Ar), 146.5 (s, C_q Ar), 146.3 (s, C_q Ar), 144.1 (C_q-Ir), 141.8 (CH Ar), 140.9 (CH Ar), 138.2 (CH Ar), 133.0 (IrC-*C*-H), 129.9, 128.8, 127.9, 127.5, 125.9, 124.5, 124.3, 122.6 (all s, CH Ar), 119.1 (C_q Ar), 111.2 (C-Br), 25.0 (s, CH_3), 23.8 (s, CH_3), 22.1 (s, CH_3). HRMS (electrospray, *m/z*) calcd. for $C_{32}H_{28}BrIrNO_2$ $[M + H]^+$: 730.0912; found: 730.0914. Anal. calcd. for $C_{32}H_{27}BrIrNO_2$ (%): C, 52.67; H, 3.73; N, 1.92. Found: C, 52.91; H, 3.78; N, 1.79. IR (cm^{-1}): ν(C=O) 1582, ν(C=C) 1533.

Preparation of Ir{κ²-*C,O*-[C(Ph)CHC(Me)O]}₂{κ²-*O,O*-[acacBr]} (11). To a stirred solution of **7** (116 mg, 0.2 mmol), in dichloromethane (3 mL), at room temperature was added dropwise a solution of *N*-bromosuccinimide (35.6 mg, 0.2 mmol) in dichloromethane (1 mL). The reaction was stirred for 1 h protected from the light, filtered through a pad of Celite, and the solvent removed *in vacuo*. The resulting red residue was washed with Et_2O (5 x 5 mL) and the residue dried *in vacuo* to give **11** as red solid (103 mg, 78%). ^{1}H NMR (400 MHz, CD_2Cl_2): δ 7.31-7.26

(overlapping signals, 6H, CH Ph), 7.22-7.19 (overlapping signals, 4H, CH Ph), 6.75 (s, IrC-C-H), 2.43 (s, 6H, CH_3), 2.38 (s, 6H, CH_3). $^{13}C\{^1H\}$ NMR (100.6 MHz, CD_2Cl_2): δ 216.6 (s, C-O furane), 211.1 (C-Ir), 184.8 (s, C-O, acac), 146.8 (s, C_q Ph), 129.6, 128.2, 126.3 (all s, CH Ph), 134.6 (s. IrC-C-H), 99.9 (s, C-Br), 23.5 (s, CH_3), 31.5 (s, CH_3). HRMS (electrospray, *m/z*) calcd. for $C_{20}H_{18}IrO_2$ $[M - Br\text{-}acac]^+$: 483.0931; found: 483.0951. Anal. calcd. for $C_{25}H_{24}BrIrO_4$ (%): C, 45.46; H, 3.66. Found: C, 45.32; H, 4.08. IR (cm^{-1}): ν(C=O) 1558, ν(C=C) 1521.

ASSOCIATED CONTENT

Supporting Information

The Supporting Information is available free of charge on the ACS Publications web site.

General information for the experimental section, structural analysis of complexes **2**, **3**, **4**, **8**, **9**, **10**, and **11**; NMR spectra; computational details; energies of calculated structures; AICD plots; NICS and NICSxx scans; and selected π molecular orbitals (PDF).

Atomic coordinates of optimized complexes (XYZ)

Accession Codes

CCDC 2270175-2270181 contain the supplementary crystallographic data for this paper. These data can be obtained free of charge via www.ccdc.cam.ac.uk/data_request/cif, or by emailing data_request@ccdc.cam.ac.uk, or by contacting The Cambridge Crystallographic Data Centre, 12 Union Road, Cambridge CB2 1EZ, UK; fax: +44 1223 336033

AUTHOR INFORMATION

Corresponding Author

* maester@unizar.es

Notes

The authors declare no competing financial interest

ACKNOWLEDGMENT

Financial support from the MICIN/AEI/10.13039/501100011033 (PID2020-115286GB-I00 and RED2022-134287-T), Gobierno de Aragón (E06_23R and LMP23_21), FEDER, and the European Social Fund is acknowledged.

REFERENCES

(1) Thorn, D. L.; Hoffmann, R. Delocalization in Metallocycles. *Nouv. J. Chim.* **1979**, *3*, 39-45.

(2) Elliott, G. P.; Roper, W. R.; Waters, J. M. Metallacyclohexatrienes or 'Metallabenzenes'. Synthesis of Osmabenzene Derivatives and X-ray Crystal Structure of [Os(CSCHCHCHCH)(CO)(PPh_3)$_2$]. *J. Chem. Soc., Chem. Commun.* **1982**, 811-813.

(3) (a) Bleeke, J. R. Metallabenzenes. *Chem. Rev.* **2001**, *101*, 1205-1228. (b) He, G.; Xia, H.; Jia, G. Progress in the Synthesis and Reactivity Studies of Metallabenzenes. *Chin. Sci. Bull.* **2004**, *49*, 1543-1553. (c) Jia, G. Progress in the Chemistry of Metallabenzynes. *Acc. Chem. Res.* **2004**, *37*, 479-486. (d) Landorf, C. W.; Haley, M. M. Recent Advances in Metallabenzene Chemistry. *Angew. Chem. Int. Ed.* **2006**, *45*, 3914-3936. (e) Jia, G. Recent progress in the chemistry of osmium carbyne and metallabenzyne complexes *Coord. Chem. Rev.* **2007**, *251*, 2167-2187. (f) Chen, J.; Jia, G. Recent development in the chemistry of transition metal-containing metallabenzenes and metallabenzynes. *Coord. Chem. Rev.* **2013**, *257*, 2491-2521. (g) Jia, G. Our Journey to the Chemistry of Metallabenzynes. *Organometallics* **2013**, *32*, 6852-6866. (h) Wright, L. J.

Metallabenzenes: An Expert View; Wiley: **2017**. (i) Zhu, C.; Xia, H. Carbolong Chemistry: A Story of Carbon Chain Ligands and Transition Metals. *Acc. Chem. Res.* **2018**, *51*, 1691-1700. (j) Wang, H.; Zhou, X.; Xia, H. Metallaaromatics Containing Main-group Heteroatoms. *Chin. J. Chem.* **2018**, *36*, 93-105. (k) Chen, D.; Hua, Y.; Xia, H. Metallaaromatic Chemistry: History and Development. *Chem. Rev.* **2020**, *120*, 12994-13086. (l) Zhang, Y.; Yu, C.; Huang, Z.; Zhang, W.-X.; Ye, S.; Wei, J.; Xi, Z. Metalla-aromatics: Planar, Nonplanar, and Spiro. *Acc. Chem. Res.* **2021**, *54*, 2323-2333. (m) Luo, M.; Chen, D.; Li, Q.; Xia, H. Unique Properties and Emerging Applications of Carbolong Metallaaromatics. *Acc. Chem. Res.* **2023**, *56*, 924-937.

(4) For some selected examples, see: (a) Paneque, M.; Posadas, C. M.; Poveda, M. L.; Rendón, N.; Salazar, V.; Oñate, E.; Mereiter, K. Formation of Unusual Iridabenzene and Metallanaphthalene Containing Electron-Withdrawing Substituents. *J. Am. Chem. Soc.* **2003**, *125*, 9898-9899. (b) Barrio, P.; Esteruelas, M. A.; Oñate, E. Preparation and Characterization of an Isometallabenzene with the Structure of a 1,2,4-Cyclohexatriene. *J. Am. Chem. Soc.* **2004**, *126*, 1946-1947. (c) Liu, B.; Xie, H.; Wang, H.; Wu, L.; Zhao, Q.; Chen, J.; Wen, T. B.; Cao, Z.; Xia, H. Selective Synthesis of Osmanaphthalene and Osmanaphthalyne by Intramolecular C-H Activation. *Angew. Chem. Int. Ed.* **2009**, *48*, 5461-5464. (d) Talavera, M.; Bolaño, S.; Bravo, J.; Castro, J.; García-Fontán, S.; Hermida-Ramón, J. M. Formation of Indanone from an Iridanaphthalene Complex. *Organometallics* **2013**, *32*, 4058-4060. (e) Fan, J.; Wang, X.; Zhu, J. Unconventional Facile Way to Metallanaphthalenes from Metal Indenyl Complexes Predicted by DFT Calculations: Origin of Their Different Thermodynamics and Tuning Their Kinetics by Substituents. *Organometallics* **2014**, *33*, 2336-2340. (f) Talavera, M.; Bravo, J.; Castro, J.; García-Fontán, S.; Hermida-Ramón, J. M.; Bolaño, S. Electronic effects of substituents on thestability of the iridanaphthalene compound [IrCp*{=C(OMe)CH=C(*o*-C_6H_4)(Ph)}(PMe_3)]PF_6. *Dalton Trans.* **2014**, *43*, 17366-

17374. (g) Vivancos, Á.; Hernández, Y. A.; Paneque, M.; Poveda, M. L.; Salazar, V.; Álvarez, E. Formation of *β*-Metallanaphthalenes by the Coupling of a Benzo-Iridacyclopentadiene with Olefins. *Organometallics* **2015**, *34*, 177-188. (h) Frogley, B. J.; Wright, L. J. Metallaanthracene and Derived Metallaanthraquinone. *Angew. Chem. Int. Ed.* **2017**, *56*, 143-147. (i) Wei, J.; Zhang, W.-X.; Xi, Z. The aromatic dianion metalloles. *Chem. Sci.* **2018**, *9*, 560-568. (j) Hu, Y. X.; Zhang, J.; Wang, X.; Lu, Z.; Zhang, F.; Yang, X.; Ma, Z.; Yin, J.; Xia, H.; Liu, S. H. One-pot syntheses of irida-polycyclic aromatic hydrocarbons. *Chem. Sci.* **2019**, *10*, 10894-10899. (k) Yu, C.; Zhong, M.; Zhang, Y.; Wei, J.; Ma, W.; Zhang, W.-X.; Ye, S.; Xi, Z. Butadienyl Diiron Complexes: Nonplanar Metalla-Aromatics Involving σ-Type Orbital Overlap. *Angew. Chem. Int. Ed.* **2020**, *59*, 19048-19053. (l) Esteruelas, M. A.; Oñate, E.; Paz, S.; Vélez, A. Repercussion of a 1,3-Hydrogen Shift in a Hydride-Osmium-Allenylidene Complex. *Organometallics* **2021**, *40*, 1523-1537. (m) Xu, B.; Mao, W.; Wu, C.; Li, J.; Lu, Z.; Luo, M.; Liu, L. L.; Mao, L.; Chen, D.; Xia, H. A One-Pot Strategy for the Synthesis of *β*-Substituted Rhoda- and Irida-Carbolong Complexes. *Chin. J. Chem.* **2022**, *40*, 1777-1784. (n) Zhang, M.-X.; Yang, X.; Xu, Z.; Yin, J.; Liu, S. H. Light- and Heat-Controlled Formation of Osmanaphthalenes and Osmanaphthalynes. *Chin. J. Chem.* **2022**, *40*, 2853-2860. (o) Wei, W.; Sung, H. H. Y.; Williams, I. D.; Jia, G. Reactions of Alkyl-Substituted Rhenacyclobutadiene Complexes with Electron-Rich Alkynes. *Eur. J. Inorg. Chem.* **2022**, e202200279. (p) Wei, W.; Xu, X.; Sung, H. H. Y.; Williams, I. D.; Lin, Z.; Jia, G. Dewar Metallabenzenes from Reactions of Metallacyclobutadienes with Alkynes. *Angew. Chem. Int. Ed.* **2022**, *61*, e202202886. (q) Li, J.; Chu, Z.; Lu, Z.; Luo, M.; Chen, D.; Xia, H. Reactivity Studies of a Hydroxy-Substituted Irida-carbolong Complex. *Organometallics* **2022**, *41*, 2589-2596. (r) Talavera, M.; Pereira-Cameselle, R.; Peña-Gallego, Á.; Vázquez-Carballo, I.; Prieto, I.; Alonso-

Gómez, J. L.; Bolaño, S. Optical and electrochemical properties of spirobifluorene iridanaphthalene complexes. *Dalton Trans.* **2023**, *52*, 487-493.

(5) (a) Bleeke, J. R.; Blanchard, J. M. B.; Donnay, E. Synthesis, Spectroscopy, and Reactivity of a Metallapyrylium. *Organometallics* **2001**, *20*, 324-336. (b) Alías, F. M.; Daff, P. J. D.; Paneque, M.; Poveda, M. L.; Carmona, E.; Pérez, P. J.; Salazar, V.; Alvarado, Y.; Atencio, R.; Sánchez-Delgado, R. C-C. Bond-Forming Reactions of Ir^{III}-Alkenyls and Nitriles or Aldehydes: Generation of Reactive Hydride- and Alkyl-Alkylidene Compounds and Observation of a Resversible 1,2-H Shift in Stable Hydride-Ir^{III} Alkylidene Complexes. *Chem. Eur. J.* **2002**, *8*, 5132-5146. (c) Esteruelas, M. A.; Fernández-Alvarez, F. J.; Oliván, M.; Oñate, E. C-H Bond Activation and Subsequent C-C Bond Formation Promoted by Osmium: 2-Vinylpyridine-Acetylene Couplings. *J. Am. Chem. Soc.* **2006**, *128*, 4596-4597. (d) Bolaño, T.; Castarlenas, R.; Esteruelas, M. A.; Oñate, E. Assembly of an Allenylidene Ligand, a Terminal Alkyne, and an Acetonitrile Molecule: Formation of Osmacyclopentapyrrole Derivatives. *J. Am. Chem. Soc.* **2006**, *128*, 3965−3973. (e) Paneque, M.; Posadas, C. M.; Poveda, M. L.; Rendón, N.; Mereiter, K. Reactivity of the Iridium(I) Alkene/Alkyne Complex $Tp^{Me2}Ir(C_2H_4)(MeO_2CC{\equiv}CCO_2Me)$ *Organometallics* **2007**, *26*, 3120-3129. (f) Buil, M. L.; Esteruelas, M. A.; Garcés, K.; Oliván, M.; Oñate, E. Understanding the Formation of N-H Tautomers from α-Substituted Pyridines: Tautomerization of 2-Ethylpyridine Promoted by Osmium. *J. Am. Chem. Soc.* **2007**, *129*, 10998-10999. (g) Esteruelas, M. A.; Masamunt, A. B.; Oliván, M.; Oñate, E.; Valencia, M. Aromatic Diosmatricyclic Nitrogen-Containing Compounds. *J. Am. Chem. Soc.* **2008**, *130*, 11612-11613. (h) Liu, B.; Wang, H.; Xie, H.; Zeng, B.; Chen, J.; Tao, J.; Wen, T. B.; Cao, Z.; Xia, H. Osmapyridine and Osmapyridinium from a Formal [4 + 2] Cycloaddition Reaction. *Angew. Chem. Int. Ed.* **2009**, *48*, 5430-5434. (i) Wang, T.; Li, S.; Zhang, H.; Lin, R.; Han, F.; Lin, Y.; Wen, T. B.; Xia, H. Annulation of

Metallabenzenes: From Osmabenzene to Osmabenzothiazole to Osmabenzoxazole. *Angew. Chem. Int. Ed.* **2009**, *48*, 6453-6456. (j) Wang, T.; Zhang, H.; Han, F.; Lin, R.; Lin, Z.; Xia, H. Synthesis and Characterization of a Metallapyridyne Complex. *Angew. Chem. Int. Ed.* **2012**, *51*, 9838-9841. (k) Alós, J.; Esteruelas, M. A.; Oliván, M.; Oñate, E.; Puylaert, P. C-H Bond Activation Reactions in Ketones and Aldehydes Promoted by POP-Pincer Osmium and Ruthenium Complexes. *Organometallics* **2015**, *34*, 4908-4921. (l) Zhou, X.; He, X.; Lin, J.; Zhuo, Q.; Chen, Z.; Zhang, H.; Wang, J.; Xia, H. Reactions of Osmium Hydrido Alkenylcarbyne with Allenoates: Insertion and [3 + 2] Annulation. *Organometallics* **2015**, *34*, 1742-1750. (m) Wang, H.; Lin, Y.-M.; Chen, S.; Ruan, Y.; Xia, H. Metallacycle Expansion and Annulation: Access to Tetrazolo-Fused Osmacycles by Reaction of Cyclic Osmium Carbyne with Sodium Azide. *Chin. J. Chem.* **2021**, *39*, 3435-3442. (n) Bai, W.; Sun, Y.; Wang, Y.; Zhou, Y.; Zhao, Y.; Bao, X.; Li, Y. An aromatic dimetallapolycyclic complex with two rhenapyrylium rings. *Chem. Commun.* **2022**, *58*, 6409-6412. (o) Shek, H.-L.; Tam, K.-T.; Yiu, S.-M.; Tse, M.-K.; Morris, R. H.; Wong, C.-Y. Osmium(II)-Induced Rearrangement of Allenols for Metallafuran Complexes. *Organometallics* **2022**, *41*, 1931-1941. (p) Cui, F.-H.; Li, Q.; Gao, L.-H.; Ruan, K.; Ma, K.; Chen, S.; Lu, Z.; Fei, J.; Lin, Y.-M.; Xia, H. Condensed Osmaquinolines with NIR-II Absorption Synthesized by Aryl C-H Annulation and Aromatization. *Angew. Chem., Int.* Ed. **2022**, *61*, e202211734. (q) Yang, X. F.; Zhang, M.-X.; Fu, D. B.; Wang, Y.; Yin, J.; Liu, S. H. Pentacyclic and Hexacyclic Osmaarynes and Their Derivatives. *Chem. Eur. J.* **2022**, *28*, e202202334. (r) Chu, Z.; Li, J.; Hua, Y.; Luo, M.; Chen, D.; Xia, H. Hetero-carbolong chemistry: experimental and theoretical studies of diaza-metallapentalenes. *Chem. Commun.* **2023**, *59*, 4173-4176.

(6) (a) Buil, M. L.; Esteruelas, M. A.; Oñate, E.; Picazo, N. R. Dissimilarity in the Chemical Behavior of Osmaoxazolium Salts and Osmaoxazoles: Two Different Aromatic

Metalladiheterocycles. *Organometallics* **2021**, *40*, 4150-4162. (b) Adamovich, V.; Benítez, M.; Boudreault, P.-L.; Buil, M. L.; Esteruelas, M. A.; Oñate, E.; Tsai, J.-Y. Alkynyl Ligands as Building Blocks for the Preparation of Phosphorescent Iridium(III) Emitters: Alternative Synthetic Precursors and Procedures. *Inorg. Chem.* **2022**, *61*, 9019-9033. (c) Benítez, M.; Buil, M. L.; Esteruelas, M. A.; Izquierdo, S.; Oñate, E.; Tsai, J.-Y. Acetylides for the Preparation of Phosphorescent Iridium(III) Complexes: Iridaoxazoles and Their Transformation into Hydroxycarbenes and *N*,*C*(sp^3),*C*(sp^2),*O*-Tetradentate Ligands. *Inorg. Chem.* **2022**, *61*, 19597-19611. (d) Buil, M. L.; Esteruelas, M. A.; Oñate, E.; Picazo, N. R. Osmathiazole Ring: Extrapolation of an Aromatic Purely Organic System to Organometallic Chemistry. *Organometallics* **2023**, *42*, 327-338

(7) (a) Fernández, I.; Frenking, G.; Merino, G. Aromaticity of metallabenzenes and related compounds. *Chem. Soc. Rev.* **2015**, *44*, 6452-6463. (b) Frogley, B. J.; Wright L. J. Recent Advances in Metallaaromatic Chemistry. *Chem. Eur. J.* **2018**, *24*, 2025-2038. (c) Chen, D.; Xie, Q.; Zhu, J. Unconventional Aromaticity in Organometallics: The Power of Transition Metals. *Acc. Chem. Res.* **2019**, *52*, 1449-1460. (d) Szczepanik, D. W.; Solà, M. Electron Delocalization in Planar Metallacycles: Hückel or Möbius Aromatic? *ChemistryOpen* **2019**, *8*, 219-227. (e) Solà, M.; Boldyrev, A. I.; Cyrañski, M. K.; Krygowski, T. M.; Merino, G. Aromaticity and Antiaromaticity: Concepts and Applications; Wiley: **2023**. (f) Merino, G.; Solà, M.; Fernández, I.; Foroutan-Nejad, C.; Lazzeretti, P.; Frenking, G.; Anderson, H. L.; Sundholm, D.; Cossío, F. P.; Petrukhina, M. A.; Wu, J.; Wu, J. I.; Restrepo, A. Aromaticity: Quo Vadis. *Chem. Sci.* **2023**, *14*, 5569-5576.

(8) (a) Rzepa, H. S.; Taylor, K. R. Möbius and Hückel spiroaromatic systems. *J. Chem. Soc., Perkin Trans.* **2002**, *2*, 1499-1501. (b) Hall, D.; Rzepa, H. S. Möbius bis and tris-spiroaromatic

systems. *Org. Biomol. Chem.* **2003**, *1*, 182-185. (c) Rzepa, H. S. Möbius Aromaticity and Delocalization. *Chem. Rev.* **2005**, *105*, 3697-3715.

(9) (a) Takase, K.; Noguchi, K.; Nakano, K. [1]Benzothiophene-Fused Chiral Spiro Polycyclic AromaticCompounds: Optical Resolution, Functionalization, and Optical Properties. *J. Org. Chem.* **2018**, *83*, 15057-15065. (b) Yang, W.-C.; Zhang, M.-M.; Feng, J.-G. Recent Advances in the Construction of Spiro Compounds via Radical Dearomatization. *Adv. Synth. Catal.* **2020**, *362*, 4446-4461. (c) Gilles, L.; Antoniotti, S. Spirocyclic Compounds in Fragrance Chemistry: Synthesis and Olfactory Properties. *ChemPlusChem* **2022**, *87*, e202200227.

(10) Zhang, Y.; Wei, J.; Chi, Y.; Zhang, X.; Zhang, W.-X.; Xi, Z. Spiro Metalla-aromatics of Pd, Pt, and Rh: Synthesis and Characterization. *J. Am. Chem. Soc.* **2017**, *139*, 5039-5042.

(11) (a) Liu, L.; Zhu, M.; Yu, H.-T.; Zhang, W.-X.; Xi, Z. Organocopper(III) Spiro Complexes: Synthesis, Structural Characterization, and Redox Transformation. *J. Am. Chem. Soc.* **2017**, *139*, 13688-13691. (b) Zhang, Y.; Wei, J.; Zhu, M.; Chi, Y.; Zhang, W.-X.; Ye, S.; Xi, Z. Tetralithio Metalla-aromatics with Two Independent Perpendicular Dilithio Aromatic Rings Spiro-fused by One Manganese Atom. *Angew. Chem., Int. Ed.* **2019**, *58*, 9625-9631.

(12) Huang, Z.; Zhang, Y.; Zhang, W.-X.; Wei, J.; Ye, S.; Xi, Z. A tris-spiro metalla-aromatic system featuring Craig-Möbius aromaticity. *Nat. Commun.* **2021**, *12*, 1319.

(13) Bai, W.; Tsang, L. Y.; Wang, Y.; Li, Y.; Sung, H. H. Y.; Williams, I. D.; Jia, G. Synthesis and characterization of bi(metallacycloprop-1-ene) complexes. *Chem. Sci.* **2023**, *14*, 96-102

(14) (a) Esteruelas, M. A.; López, A. M.; Oliván, M. Osmium-carbon double bonds: Formation and reactions. *Coord. Chem. Rev.* **2007**, *251*, 795-840. (b) He, G.; Chen, J.; Xia, H. Metallafurans and their synthetic chemistry. *Sci. Bull.* **2016**, *61*, 430-442.

(15) Li, X.; Vogel, T.; Incarvito, C. D.; Crabtree, R. H. Electronic and Steric Effects in the Insertion of Alkynes into an Iridium(III) Hydride. *Organometallics* **2005**, *24*, 62-76.

(16) Buil, M. L.; Esteruelas, M. A.; Garcés, K.; Oliván, M.; Oñate, E. Cβ(sp^2)-H Bond Activation of α,β-Unsaturated Ketones Promoted by a Hydride-Elongated Dihydrogen Complex: Formation of Osmafuran Derivatives with Carbene, Carbyne, and NH-Tautomerized α-Substituted Pyridine Ligands. *Organometallics* **2008**, *27*, 4680-4690.

(17) (a) Schleyer, P. v. R.; Pühlhofer, F. Recommendations for the Evaluation of Aromatic Stabilization Energies. *Org. Lett.* **2002**, *4*, 2873-2876. (b) Wannere, C. S.; Schleyer, P. v. R. How Aromatic Are Large (4n+2)π Annulenes? *Org. Lett.* **2003**, *5*, 2983-2986. (c) Fernández, I.; Frenking, G. Direct Estimate of Aromaticity with the Energy Decomposition Analysis. *Open Org. Chem. J.* **2011**, *5*, 79-86.

(18) Chen, Z.; Wannere, C. S.; Corminboeuf, C.; Puchta, R.; Schleyer, P. v. R. Nucleus-Independent Chemical Shifts (NICS) as an Aromaticity Criterion. *Chem. Rev.* **2005**, *105*, 3842-3888.

(19) Geuenich, D.; Hess, K.; Köhler, F.; Herges, R. Anisotropy of the Induced Current Density (ACID), a General Method To Quantify and Visualize Electronic Delocalization. *Chem. Rev.* **2005**, *105*, 3758-3772.

(20) (a) Mayer, I. Bond order and valence indices: A personal account. *J. Comput. Chem.* **2007**, *28*, 204-221. (b) Benitez, D.; Shapiro, N. D.; Tkatchouk, E.; Wang, Y.; Goddard III, W. A.; Toste, F. D. A bonding model for gold(I) carbene complexes. *Nat. Chem.* **2009**, *1*, 482-486.

(21) (a) Wen, T. B.; Ng, S. M.; Hung, W. Y.; Zhou, Z. Y.; Lo, M. F.; Shek, L.-Y.; Williams, I. D.; Lin, Z.; Jia, G. Protonation and Bromination of an Osmabenzyne: Reactions Leading to the Formation of New Metallabenzynes. *J. Am. Chem. Soc.* **2003**, *125*, 884-885. (b) Hung, W. Y.; Liu, B.; Shou, W.; Wen, T. B.; Shi, C.; Sung, H. H.-Y.; Williams, I. D.; Lin, Z.; Jia, G. Electrophilic Substitution Reactions of Metallabenzynes. *J. Am. Chem. Soc.* **2011**, *133*, 18350-18360. (c) Clark, G. R.; Johns, P. M.; Roper, W. R.; Söhnel, T.; Wright, L. J. Regioselective Mono-, Di-, and Trifunctionalization of Iridabenzofurans through Electrophilic Substitution Reactions. *Organometallics* **2011**, *30*, 129-138. (d) Bai, W.; Lee, K.-H.; Hung, W. Y.; Sung, H. H. Y.; Williams, I. D.; Lin, Z.; Jia, G. Reactions of Osmium Carbyne Complexes $OsCl_3(\equiv CR)(PPh_3)_2$ (R = $CH{=}CPh_2$, CH_2Ar) with Bromine and Hydrogen Peroxide. *Organometallics* **2017**, *36*, 657-664. (e) Zhou, X.; Zhang, H. Reactions of Metal-Carbon Bonds within Six-Membered Metallaaromatic Rings. *Chem. Eur. J.* **2018**, *24*, 8962-8973. (f) Li, J.; Lu, Z.; Hua, Y.; Chen, D.; Xia, H. Carbolong chemistry: nucleophilic aromatic substitution of a triflate functionalized iridapentalene. *Chem. Commun.* **2021**, *57*, 8464-8467. (g) Cai, Y.; Hua, Y.; Lu, Z.; Lan, Q.; Lin, Z.; Fei, J.; Chen, Z.; Zhang, H.; Xia, H. Electrophilic aromatic substitution reactions of compounds with Craig-Möbius aromaticity. *PNAS* **2021**, *118*, e2102310118. (h) Chu, Z.; Li, J.; Chen, D.; Lu, Z.; Meng, W.; Luo, M.; Xia, H. Formal [2+1] Cycloadditions of a Metallacyclopentadiene Unit with Alkynes: Constructing Tetracyclic Conjugated Frameworks with Bridgehead Metals. *Chin. J. Chem.* **2023**, *41*, 1987-1993.

(22) (a) Olah, G. A. Mechanism of Electrophilic Aromatic Substitutions. *Acc. Chem. Res.* **1971**, *4*, 240-248. (b) Mąkosza, M. Electrophilic and Nucleophilic Aromatic Substitutions are Mechanistically Similar with Opposite Polarity. *Chem. Eur. J.* **2020**, *26*, 15346-15353.

(23) (a) Corbet, J.-P.; Mignani, G. Selected Patented Cross-Coupling Reaction Technologies. *Chem. Rev.* **2006**, 106, 2651-2710. (b) Johansson Seechurn, C. C. C.; Kitching, M. O.; Colacot, T. J.; Snieckus, V. Palladium-Catalyzed Cross-Coupling: A Historical Contextual Perspective to the 2010 Nobel Prize. *Angew. Chem. Int. Ed.* **2012**, *51*, 5062-5085. (c) Campeau, L.-C.; Hazari, N. Cross-Coupling and Related Reactions: Connecting Past Success to the Development of New Reactions for the Future. Organometallics **2019**, *38*, 3-35. (d) Kadu, B. S.; Suzuki–Miyaura cross coupling reaction: recent advancements in catalysis and organic synthesis. *Catal. Sci. Technol.* **2021**, *11*, 1186-1221

(24) Saikia, I.; Borah, A. J.; Phukan, P. Use of Bromine and Bromo-Organic Compounds in Organic Synthesis. *Chem. Rev.* **2016**, *116*, 6837-7042.

(25) Alvarez-Idaboy, J. R.; Montero, L. A.: Martínez, R. An Application of Theoretical Models to Understand Chemical Reactions: The Electrophilic Substitution in Furan. In: Montero, L.A., Smeyers, Y. G. (Eds.) Trends in Applied Theoretical Chemistry. Topics in Molecular Organization and Engineering, 1992, vol 9. Springer, Dordrecht. (https://doi.org/10.1007/978-94-011-2498-0_4).

(26) Buil, M. L.; Esteruelas, M. A.; López, A. M. Recent Advances in Synthesis of Molecular Heteroleptic Osmium and Iridium Phosphorescent Emitters. *Eur. J. Inorg. Chem.* **2021**, 4731-4761.

(27) Sprouse, S.; King, K. A.; Spellane, P. J.; Watts, R. J. Photophysical Effects of Metal-Carbon Bonds in Ortho-Metalated Complexes of Ir(III) and Rh(III). *J. Am. Chem. Soc.* **1984**, *106*, 6647-6653.

(28) (a) Lamansky, S.; Djurovich, P.; Murphy, D.; Abdel-Razzaq, F.; Kwong, R.; Tsyba, I.; Bortz, M.; Mui, B.; Bau, R.; Thompson, M. E. Synthesis and Characterization of Phosphorescent Cyclometalated Iridium Complexes. *Inorg. Chem.* **2001**, *40*, 1704-1711. (b) Huo, S.; Deaton, J. C.; Rajeswaran, M.; Lenhart, W. C. Highly Efficient, Selective, and General Method for the Preparation of Meridional Homo- and Heteroleptic Tris-cyclometalated Iridium Complexes *Inorg. Chem.* **2006**, *45*, 3155-3157. (c) Baranoff, E.; Curchod, B. F. E.; Frey, J.; Scopelliti, R.; Kessler, F.; Tavernelli, I.; Rothlisberger, U.; Grätzel, M.; Nazeeruddin, M. K. Acid-Induced Degradation of Phosphorescent Dopants for OLEDs and Its Application to the Synthesis of Tris-heteroleptic Iridium(III) Bis-cyclometalated Complexes. *Inorg. Chem.* **2012**, *51*, 215-224. (d) Kim, T.; Kim, H.; Lee, K. M.; Lee, Y. S.; Lee, M. H. Phosphorescence Color Tuning of Cyclometalated Iridium Complexes by *o*-Carborane Substitution. *Inorg. Chem.* **2013**, *52*, 160-168. (e) Pal, A. K.; Henwood, A. F.; Cordes, D. B.; Slawin, A. M. Z.; Samuel, I. D. W.; Zysman-Colman, E. Blue-to-Green Emitting Neutral Ir(III) Complexes Bearing Pentafluorosulfanyl Groups: A Combined Experimental and Theoretical Study. *Inorg. Chem.* **2017**, *56*, 7533-7544. (f) Kim, J.-H.; Kim, S.-Y.; Jang, S.; Yi, S.; Cho, D. W.; Son, H.-J.; Kang, S. O. Blue Phosphorescence with High Quantum Efficiency Engaging the Trifluoromethylsulfonyl Group to Iridium Phenylpyridine Complexes. *Inorg. Chem.* **2019**, 58, 16112-16125. (g) Lorenzo-Aparicio, C.; Gómez Gallego, M.; Ramírez de Arellano, C.; Sierra, M. A. Phosphorescent Ir(III) complexes derived from purine nucleobases *Dalton Trans.* **2022**, *51*, 5138-5150.

(29) The structure of complex **4** has two chemically equivalent but crystallographically independent cations and anions in the asymmetric unit, while the structure of derivative **8** has two chemically equivalent but crystallographically independent molecules in the asymmetric unit.

(30) See, for example: (a) Wang, B.-Y.; Karikachery, A. R.; Li, Y.; Singh, A.; Lee, H. B.; Sun, W.; Sharp, P. R. Remarkable Bromination and Blue Emission of 9-Anthracenyl Pt(II) Complexes. *J. Am. Chem. Soc.* **2009**, *131*, 3150′-3151. (b) Karikachery, A. R.; Masjedi, M.; Sharp, P. R. Thermal and Photochemical Ring-Bromination in Naphthyl-, Naphthdiyl-, and Dicarboximideperyl-Platinum Complexes. *Organometallics* **2015**, *34*, 1635-1642.

(31) (a) Koval, I. V. *N*-Halo Reagents. *N*-Halosuccinimides in Organic Synthesis and in Chemistry of Natural Compounds. *Russ. J. Org. Chem.* **2002**, *38*, 301-337. (b) Saikia, I.; Borah, A. J.; Phukan, P. Use of Bromine and Bromo-Organic Compounds in Organic Synthesis. *Chem. Rev.* **2016**, *116*, 6837-7042. (c) Das, R.; Kapur, M. Transition-Metal-Catalyzed Site-Selective C-H Halogenation Reactions. *Asian J. Org. Chem.* **2018**, *7*, 1524-1541. (d) Baker, S. I.; Yaghoubi, M.; Bidwell, S. L.; Pierce, S. L.; Hratchian, H. P.; Baxter, R. D. Enhanced Reactivity for Aromatic Bromination via Halogen Bonding with Lactic Acid Derivatives. *J. Org. Chem.* **2022**, *87*, 8492-8502.

(32) (a) Yu, Q.; Hu, L. A.; Wang, Y.; Zheng, S.; Huang, J. Directed *meta*-Selective Bromination of Arenes with Ruthenium Catalysts. *Angew. Chem. Int. Ed.* **2015**, *54*, 15284-15288. (b) Warratz, S.; Burns, D. J.; Zhu, C.; Korvorapun, K.; Rogge, T.; Scholz, J.; Jooss, C.; Gelman, D.; Ackermann, L. *meta*-C-H Bromination on Purine Bases by Heterogeneous Ruthenium Catalysis. *Angew. Chem. Int. Ed.* **2017**, *56*, 1557-1560.

(33) Boudreault, P.-L. T.; Esteruelas, M. A.; Mora, E.; Oñate, E.; Tsai, J.-Y. Bromination and C-C Cross-Coupling Reactions for the C-H Functionalization of Iridium(III) Emitters. *Organometallics* **2021**, *40*, 3211-3222.

(34) (a) Shernyukov, A. V.; Genaev, A. M.; Salnikov, G. E.; Shubina, V. G.; Rzepa, H. S. Elevated reaction order of 1,3,5-tri-*tert*-butylbenzene bromination as evidence of a clustered polybromide transition state: a combined kinetic and computational study. *Org. Biomol. Chem.* **2019**, *17*, 3781-3789. (b) Hou, H.-X.; Zhou, D.-G.; Li, R. Mechanisms of bromination between thiophenes and NBS: A DFT investigation. *Comput. Theor. Chem.* **2022**, *1208*, 113545.

(35) van der Ent, A.; Onderdelinden, A. L.; Schunn, R. A. Chlorobis(cyclooctene)rhodium(I) and -iridium(I) complexes. *Inorg. Synth.* **2007**, *28*, 90-92.

For Table of Contents Only

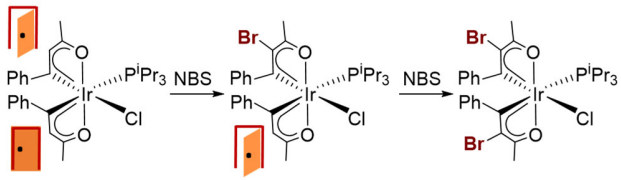

Synopsis

A family of spiro iridafurans has been prepared. They result from the activation of the Cβ(sp^2)-H bond of two benzylideneacetone molecules at an iridium center. The aromaticity of iridafuran moiety has been evaluated by experimental criteria and computational methods (AICD, NICS, ASE and NBO) and confirmed by selective bromination reactions, with *N*-bromosuccinimide, which depend on the ligands arranged trans to the carbons attached to the metal.